Marine Geology 443 (2022) 106697

Contents lists available at ScienceDirect

Marine Geology

journal homepage: www.elsevier.com/locate/margo

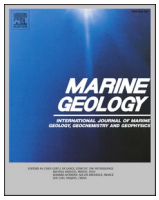

Source-to-sink pathways of clay minerals in the cadiz contourite system over the last 25 kyrs: The segregational role of mediterranean outflow water

Paul Moal-Darrigade [a,*], Emmanuelle Ducassou [a], Viviane Bout-Roumazeilles [b], Vincent Hanquiez [a], Marie-Claire Perello [a], Thierry Mulder [a], Jacques Giraudeau [a]

[a] Université de Bordeaux, UMR CNRS 5805 EPOC, Allée Geoffroy St Hilaire, 33615 Pessac, France
[b] Université Lille 1, Laboratoire Géosystèmes, UMR 8217 CNRS, bâtiment SN5, Villeneuve d'Ascq cedex, France

ARTICLE INFO

Editor: Michele Rebesco

Keywords:
Clay minerals
Mediterranean outflow
Source-to-sink
Contourite
Bottom current
Late quaternary

ABSTRACT

Despite major advances in our understanding of the interactions between bottom currents and sedimentary deposits over the last forty years, few studies have focused on the nature of fine particles in contourite depositional systems (CDS). XRD analyses of marine sediments can be used to improve our understanding of fine-grained sediment sources and settling processes. This work presents a detailed sedimentological study of sediment cores collected over the middle slope of the Gulf of Cadiz as part of Integrated Ocean Drilling Program Expedition 339 and the 2001 CADISAR cruise. We performed high-resolution clay mineral analyses to reconstruct the pathways of fine-grained particles from their sources to their deposition along the contourite depositional system of the Gulf of Cadiz (source-to-sink approach). The clay mineral associations reflect the major contribution of the Guadalquivir River and North African rivers/dusts to fine particles settling over the middle slope. Our results suggest that size segregation deposition processes along the path of the Mediterranean Outflow Water (MOW) are responsible for the distinct clay mineral associations between sites located under the upper MOW and the lower MOW. We observed changes of sedimentation rates over the contourite depositional system throughout the last 25 kyrs. We propose that these changes are due to temporal variations in the vertical distribution of the upper and the lower MOW whose concentrations in suspended particulate matter are drastically different. Sea-level and large scale atmospheric changes (e.g., ITCZ migration) over this period induced major variations in the distance of river mouths to the Gulf of Cadiz CDS, and in the amount of Northwest African dust delivered to this depositional system, respectively. Climate changes therefore modified fine particle sources and pathways, which considerably influenced clay minerals settling in the middle slope of the Gulf of Cadiz since the Last Glacial Maximum.

1. Introduction

The 350 km-long margin of the Gulf of Cadiz, extending from the entrance of Atlantic water through the Strait of Gibraltar to Cape St. Vincent, has a curved shape due to tectonic features (Baldy et al., 1977; Maldonado et al., 1999; Nelson and Maldonado, 1999). The shelf break, located at 120–140 m water depth, marks the boundary between the continental shelf and the slope (10–30 km; López-Galindo et al., 1999; Hernández-Molina et al., 2006). Between 130 and 4000 m water depth, the continental slope dips gently between 0.5° and 4° (Hernández-Molina et al., 2006; and references therein). The special feature of this margin is the extensive middle slope Contourite Depositional System (CDS) which is strongly influenced by the Mediterranean Outflow Water (MOW) (e.g., Hernández-Molina et al., 2006). This CDS consists of numerous large contourite accumulations, named drifts (McCave and Tucholke, 1986), along with erosional features such as moat and contourite channels.

For several decades, great efforts have been devoted to the study of the depositional model of the Gulf of Cadiz CDS. This body of work demonstrated both the importance of recent tectonic activity, which influenced the morphology of the middle slope (Llave et al., 2001, 2007; García et al., 2009, 2016, 2020; Medialdea et al., 2009; Hernández-

* Corresponding author.
E-mail address: paul.moal@u-bordeaux.fr (P. Moal-Darrigade).

https://doi.org/10.1016/j.margeo.2021.106697
Received 12 February 2021; Received in revised form 24 September 2021; Accepted 8 November 2021
Available online 15 November 2021

Molina et al., 2016), and the pivotal role of alongslope processes, induced by the MOW (e.g., Kenyon and Belderson, 1973; Faugères et al., 1984; Gonthier et al., 1984; Stow et al., 1986; Stow et al., 2013a; Habgood et al., 2003; Hernández-Molina et al., 2003, 2006; Hanquiez et al., 2007; Marchès et al., 2007; García et al., 2009; Roque et al., 2012). Furthermore, downslope processes interact with alongslope processes (e.g., Mulder et al., 2013; De Castro et al., 2020, 2021) but they are less noticeable and less continuous over the CDS than the contourite deposits (Hernández-Molina et al., 2006).

The MOW splits into two main cores when it enters the Gulf of Cadiz: the shallow upper MOW (300–800 m) which circulates along the base of the upper slope and the lower MOW which flows along the base of the middle slope (Fig. 1A, Sánchez-Leal et al., 2017). Marine geological studies based on sediment cores and IODP sites collected over different contourite drifts have highlighted fluctuations of MOW velocities and vertical oscillations of its core depth during the late Pleistocene. It is considered that MOW flows at shallower depths during interglacial warm conditions than during glacial cold periods (Schönfeld and Zahn, 2000; Rogerson et al., 2005; Llave et al., 2006). Strengthening of the MOW occurs during colder conditions such as the Younger Dryas, and Heinrich stadials and stadials of interglacials including Dansgaard-Oeschger cold events (Sierro et al., 1999; Cacho et al., 2000; Mulder et al., 2002; Llave et al., 2006; Voelker et al., 2006; Toucanne et al., 2007; Bahr et al., 2014). Furthermore, the enhanced run-off into the

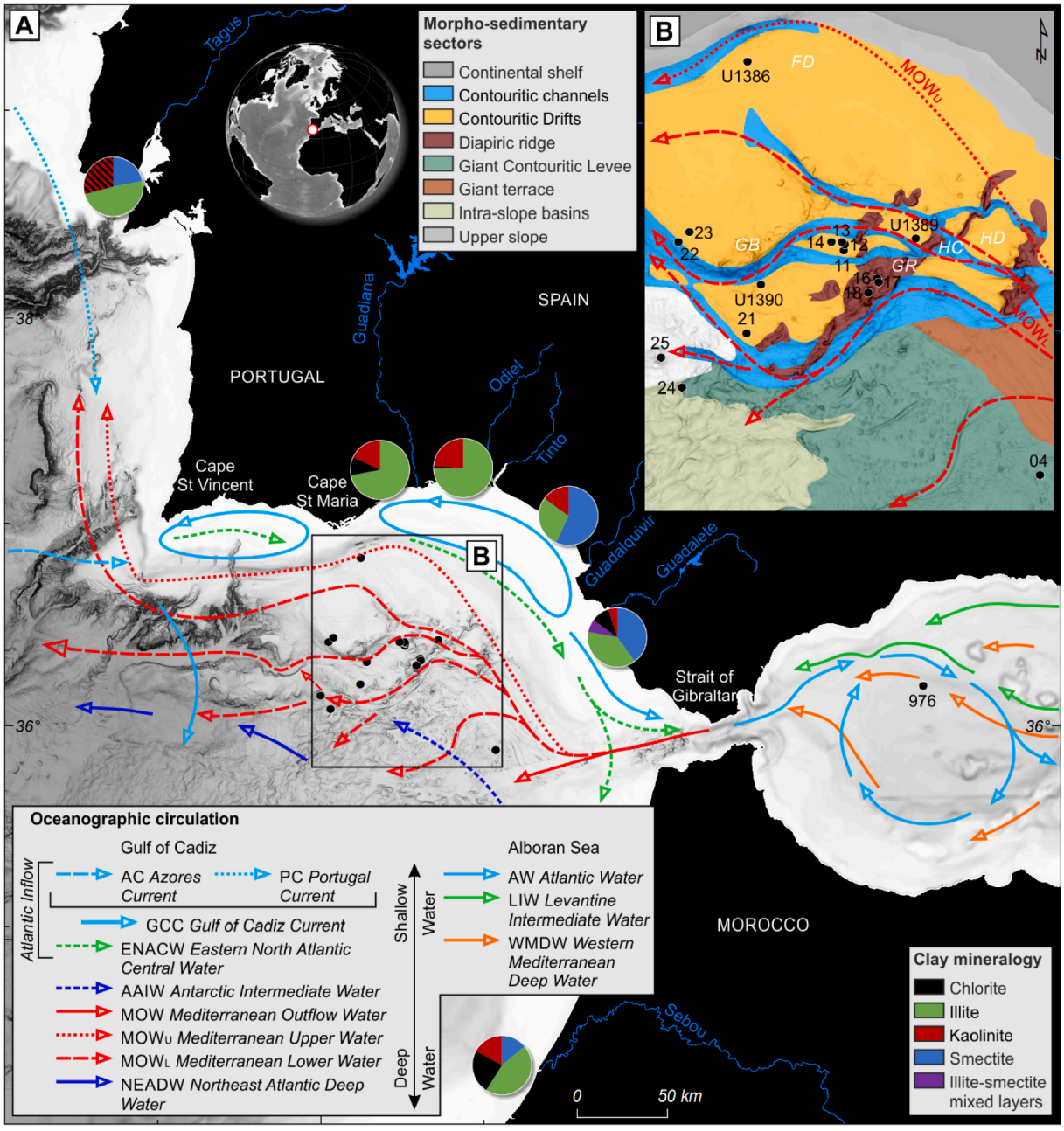

Fig. 1. A) General currents and water masses in the Gulf of Cadiz (García-Lafuente et al., 2006; Voelker et al., 2010; Carracedo et al., 2016; Hernández-Molina et al., 2016), Alboran Sea (Ercilla et al., 2016) and southwestern Portuguese margin (Teixeira et al., 2019; Rodrigues et al., 2020), clay mineralogy of the main south-western Iberian and Moroccan rivers and location of ODP Site 976 (Lima, 1971; Mélières, 1973; Fernández-Caliani et al., 1997; López-Galindo et al., 1999; Elmouden et al., 2005; Gutiérrez-Mas et al., 2006; Machado et al., 2007; Achab et al., 2008). B) Main morpho-sedimentary features of the Gulf of Cadiz CDS (Hernández-Molina et al., 2006), locations of IODP Sites and CADISAR cores used this study and pathways of the upper branch (MOW_U) and lower branch (MOW_U) of Mediterranean Outflow Water (MOW). FD: Faro Drift; HD: Huelva Drift; HC: Huelva Channel; GR: Guadalquivir Ridge; GB: Guadalquivir Bank.

Eastern Mediterranean Sea during periods of maximum summer insolation prevented Eastern Mediterranean deep water formation (Rogerson et al., 2012; Rohling et al., 2015), inducing sapropel deposition in the Mediterranean and a weak activity of the MOW (Rogerson et al., 2012; Bahr et al., 2015; Kaboth et al., 2016). Therefore, the nature, dynamics and feedback mechanisms between past variations in intensity and depth of MOW and climatic conditions are still debated.

As sand and silt content is a key indicator of bottom current velocity, mostsedimentological work concerning the Gulf of Cadiz CDS has focused on coarse-grained sediment deposition, in particular through the extensive study of sandy-contourites (e.g., Stow et al., 2013b; Brackenridge et al., 2018; De Castro et al., 2021); whereas few studies have focussed on muddy intervals (Nishida, 2016). Some authors have investigated the mineralogy of clays from the middle slope of the Gulf of Cadiz (Grousset et al., 1988; Stumpf et al., 2011; Alonso et al., 2016), often with a low temporal resolution, but little attention has been paid to the spatial distribution of clay minerals among muddy-contourites of the CDS. By contrast, the pattern of clay mineral distribution on the shelf of the Gulf of Cadiz has been the subject of many studies and it is very well constrained (Fernández-Caliani et al., 1997; Gutiérrez-Mas et al., 1997; Gutiérrez-Mas et al., 2003; Gutiérrez-Mas et al., 2006; López-Galindo et al., 1999; Machado, 2005; Machado et al., 2007; Achab et al., 2008; Achab, 2011). The present study investigates clay mineralogy of sediments from three IODP sites and thirteen sediment cores collected across various sedimentary features of the Gulf of Cadiz in order to reconstruct the source-to-sink pathway of clay minerals from their sources (river/wind) to their deposition in the CDS of the Gulf of Cadiz. The substantial clay mineral dataset produced in this study contributes to: 1) identifying the fluvial and eolian sources of clay minerals of the middle slope in the Gulf of Cadiz and quantifying their respective contributions to sedimentation; 2) highlighting the strong role of surface currents and of the MOW with specific emphases on its upper and lower components in the distribution of clay minerals along the CDS; 3) pointing out changes in both clay mineral sources and transport patterns in the CDS over the last 25 kyrs.

2. Regional setting

2.1. Morphobathymetric setting

The northern continental shelf of the Gulf of Cadiz is located between the Iberian Peninsula and Morocco, west of the Strait of Gibraltar (Fig. 1A). This 350-km long continental margin extends from the Strait of Gibraltar to the Cape St Vincent, and is characterized by a unique continental slope (Fig. 1A). The interaction between Mediterranean Outflow Water (MOW) and the seafloor across the slope generates one of the most studied Contourite Depositional Systems (CDS) in the world (Hernández-Molina et al., 2003). The Gulf of Cadiz CDS, located over the middle slope (400–1200 m) encompasses five morphobathymetric sectors, identified according to distinct sedimentary features (Hernández-Molina et al., 2006). In the souteast area, the proximal scour and sand-ribbon sector is dominated by erosive features (e.g., Kenyon and Belderson, 1973; Hernández-Molina et al., 2003, 2006; García et al., 2009; Stow et al., 2013a). The adjacent overflow-sedimentary lobe sector (Fig. 1B) displays a large sand and mud sedimentary lobe impacted by both depositional and erosive processes (Kenyon and Belderson, 1973; Habgood et al., 2003; Hernández-Molina et al., 2003; Mulder et al., 2003; Hanquiez et al., 2010). Located in the central area of the middle slope between Cadiz and Faro, the channel and ridge sector (Fig. 1B) is characterized by five main contourite channels (Cadiz, Guadaquivir, Huelva, Diego Cao and Gusano) dominated by erosive processes (Nelson et al., 1993; García, 2002; García et al., 2009). These different contourite channels cross a depositional sector composed of active (Huelva Drift and Guadalquivir Drift) and buried drifts (Mulder et al., 2002; Hanquiez et al., 2007; Llave et al., 2007; García et al., 2009). In addition, erosive channels circumvent marked structural reliefs of diapiric ridges and banks (e.g., Guadalquivir Ridge and Bank; Hernández-Molina et al., 2003, 2006; Hanquiez et al., 2007; García et al., 2009). In the active contourite deposition sector, which is located in the northwest of the area (Fig. 1B), depositional features represented by contourite drifts (e.g., Faro Drift) dominate the sedimentation regime (e.g., Gonthier et al., 1984; Faugères et al., 1984; Stow et al., 1986; Mulder et al., 2002; Hernández-Molina et al., 2003; Llave et al., 2006; Roque et al., 2012). A series of canyons, namely Portimao, Lagos, Sagres and San Vicente Canyons, are located in the western sector (the canyon sector) of the study area (Fig. 1B) (e.g., Hernández-Molina et al., 2003; Mulder et al., 2006; Llave et al., 2007; Marchès et al., 2007).

The present study especially focuses on the Faro elongated and separated mounded Drift, the Huelva mounded Drift and the large sheeted drift located southeast of the Guadalquivir Bank (Fig. 1B). These drift drilled by the Integrated Ocean Drilling Program (IODP) Expedition 339 (Hernández-Molina et al., 2013; Stow et al., 2013b). A further thirteen piston cores from the CADISAR cruise collected over the channel/ridge and overflow-sedimentary lobe sectors complemented this work.

2.2. Oceanographic circulation

The oceanographic circulation in the Gulf of Cadiz is driven by the inflow-outflow circulation across the Strait of Gibraltar, with Atlantic water entering in the Mediterranean Sea at the surface and Mediterranean intermediate and deep waters outflowing westward below 150 m water depth (Ambar and Howe, 1979; Bryden and Stommel, 1984; Ochoa and Bray, 1991; Bryden et al., 1994; Baringer and Price, 1999; Millot, 1999; Pinardi et al., 2019). At the exit of the Strait of Gibraltar (Fig. 1A), MOW is principally composed of Levantine Intermediate Water (LIW) with a small contribution of Western Mediterranean Deep Water (WMDW) (Ambar and Howe, 1979; Bryden and Stommel, 1984; Millot, 2014). In the Gulf of Cadiz, the dense cascading MOW splits into two main cores (Fig. 1B): (1) the Mediterranean upper water (MOW_U) which flows along the base of the upper slope between 300 and 800 m, and mixes with the overlaying warmer upper water of the Eastern North Atlantic Central Water (ENACW; Ambar et al., 2002; Bellanco and Sánchez-Leal, 2016; Sánchez-Leal et al., 2017); and (2) the Mediterranean lower water (MOW_L) which flows at deeper depth (800–1200 m), overlies Labrador Sea Water (LSW) and northeast Atlantic deep water (NEADW), and is underlaid by northward flowing Antarctic Intermediate Water (AAIW) in the south area of the Gulf of Cadiz (Fig. 1A; Voelker, 2015; Carracedo et al., 2016; Roque et al., 2019). MOW velocity gradually decreases northwestward from ca. 300 cm s^{-1} in the Strait of Gibraltar to 15–20 cm s^{-1} near Cape St. Vincent (Ambar and Howe, 1979; Gasser et al., 2017; Sánchez-Leal et al., 2017).

The surficial circulation in the Gulf of Cadiz in the upper ~150 m is mainly driven by the eastern branch of the Azores Current (AC) and the Portugal Current (PC; Fig. 1.A) advecting subtropical salty water and less salty, cooler water, respectively (Peliz et al., 2005; García-Lafuente et al., 2006). Closer to the shore, two shallow cyclonic cells borderthe open ocean: one located to the south of Cape St. Maria, namely the eddy of Cape St. Maria, the other forming between Cape St. Monica and the Guadalquivir River mouth in the eastern sector of the shelf (Fig. 1A). The latter occurs as the westward flowing Cadiz Coastal Counter Current meets the Gulf of Cadiz Current (GCC) flowing toward the Strait of Gibraltar (Relvas and Barton, 2002; García-Lafuente et al., 2006).The Atlantic inflow into the western Mediterranean Sea contains water from both AC and GCC (Peliz et al., 2009).

2.3. Clay mineral sources

Recent sedimentation in the Gulf of Cadiz is largely dominated by terrigenous material from the vicinity of the Iberian margin and North African continent (Milliman and Syvitski, 1992; Gutiérrez-Mas et al., 1997, 2003, 2006; Achab et al., 2008; Achab, 2011). In this context,

fine-grained detrital particles are supplied to the ocean by either (1) rivers (Grousset et al., 1988; Morales, 1997; López-Galindo et al., 1999) or (2) eolian transport (Moreno et al., 2002; Stuut et al., 2009; Bout-Roumazeilles et al., 2013; Stumpf et al., 2011), before being further advected or redistributed as suspended particulate matter (SPM) by (3) ocean currents and sedimentary processes (Pierce and Stanley, 1975; Grousset et al., 1988; Morales, 1997; Baringer and Price, 1999).

The Guadalquivir River ($5.9*10^6$ t yr^{-1}), the Guadiana River ($2.9*10^6$ t yr^{-1}) and the Tinto-Odiel Rivers system ($0.65*10^6$ t yr^1) are the main fluvial contributors (Fig. 1A) to clay sedimentation in the Gulf of Cadiz (Van Geen et al., 1997; Elbaz-Poulichet et al., 2001; Lobo et al., 2001; Machado et al., 2007). However, additional contributions from the Guadelete and Sanctipetri rivers (unknown annual sediment discharge but low daily mean flow of 16.2 m^3 s^{-1}; Solari et al., 2017), from the western Portuguese Tagus and Sado Rivers (up to $\sim 1*10^6$ t yr^{-1}) or the Moroccan Sebou and Loukkos rivers (Vale and Sundby, 1987; Jouanneau et al., 1998; Freitas et al., 1998; Oliveira et al., 2002; Palma et al., 2012; Fernández-Nóvoa et al., 2017) cannot be ruled out (Fig. 1A).

Eolian supply is estimated to be as important to the Gulf of Cadiz as it is to the Western Mediterranean Sea ($3.9*10^6$ t yr^{-1}). Wind transport of fine material take place essentially via the northern branch of the Saharan Air Layer (Guerzoni et al., 1997; Goudie and Middleton, 2001; Bout-Roumazeilles et al., 2007), with some regional supply from the Iberian Peninsula (Moulin et al., 1997; Moreno et al., 2002).

Redistribution of terrigenous fine-grained particles is a dominant process in the Gulf of Cadiz with a main east-southeastward pathway via surface currents and along-slope transport by the Atlantic Inflow (Gutiérrez-Mas et al., 1997, 2006). In addition, a westward advection of SPM from the Alboran Sea occurs at deeper depth via the Mediterranean Outflow Water (Pierce and Stanley, 1975; Grousset et al., 1988; Baringer and Price, 1999). Some across-slope transfers of detrital particles resulting from gravity processes likely contribute to sedimentation in the Gulf of Cadiz (Alonso et al., 2016; De Castro et al., 2021).

The nature and composition of the clay mineral assemblage largely reflect the main geological characteristics of rocks and soils outcropping in the deflation basin for eolian dust or in the drainage basin for river-borne particles modified by regional environmental conditions (erosion versus physical weathering, hydrolysis; e.g., Chamley, 1989). From west to east, the Guadiana River and the Tinto-Odiel rivers mainly drain the Iberian massif (Sierra Morena), the Guadalquivir River drains both metamorphic and sedimentary rocks of the Betic Range and post-orogenic sedimentary rocks, while the Guadalete River and the Sanctipetri River run across the external domains of the Betic Cordilleras. The clay mineral assemblages in sediments from the Gulf of Cadiz have been extensively studied over the last decades (Mélières, 1973; Auffret et al., 1974; Pierce and Stanley, 1975; Grousset et al., 1988; Fernández-Caliani et al., 1997; Gutiérrez-Mas et al., 1997, 2003, 2006; Elbaz-Poulichet et al., 2001; Lobo et al., 2001; Machado, 2005; Achab et al., 2008). On average, recent sub-surface sediments are dominated by abundant illite (60%) associated with 20% smectite and expandable mixed layers. Chlorite and kaolinite represent together around 20% of the clay mineral assemblage while palygorskite occurs as trace amounts (<5%).

2.3.1. Illite and chlorite

As close analogues of mica, illite and chlorite are generally considered to be detrital, directly resulting from physical erosion of crustal and metamorphic rocks (Chamley, 1989). In the Gulf of Cadiz, abundant inherited illite reflects the regional geological settings and composition of the main river watershed areas (Fig. 1A; Gutiérrez-Mas et al., 1997; Machado et al., 2007). The Guadiana (64–72% illite and 9–12% chlorite) and Tinto-Odiel rivers (up to 80% illite), which drain Paleozoic and metamorphic cratonic block, are responsible for the dominant illite and chlorite supply to the Gulf of Cadiz (Fernández-Caliani et al., 1997; Gonzalez et al., 2004; Machado, 2005; Machado et al., 2007; Morales et al., 2006).

The Guadalquivir River is the second most important supplier of illite (40%) to deep-sea sedimentation. Local enrichment of illite versus smectite on the nearby continental shelf (up to 60%) is interpreted as the result of both additional supply by the Guadiana and Tinto-Odiel rivers and of differential settling processes (López-Galindo et al., 1999; Gutiérrez-Mas et al., 2003, 2006; Achab et al., 2008). Indeed, differential sedimentation may modify the distribution of some clay minerals (smectite and kaolinite versus illite; Mélières, 1973; Fernández-Caliani et al., 1997; Gutiérrez-Mas et al., 2006). The Guadalete River transports up to 40% of low-crystalline illite derived from the Betic Cordilleras contrasting with the high-crystalline illite transported by the Guadalquivir River—and ~ 10% of chlorite (López-Galindo et al., 1999; Gutiérrez-Mas et al., 2006; Achab et al., 2008).

Though remote, the Tagus and Sado Rivers and the NW Spanish and West Portuguese margins must be considered as potential sources of illite to the Gulf of Cadiz via surface currents (Freitas et al., 1998; Oliveira et al., 2002). Similarly, the Sebou River off the Moroccan margin is a potential source of illite (40–70%) and chlorite (13–27%) to the Gulf of Cadiz (Snoussi, 1986; Grousset et al., 1988; Elmouden et al., 2005; Palma et al., 2012). Illite can also be supplied via eolian processes since illite is a major component of dust originating from the Moroccan Atlas (66%) and Central Sahara (52–60%) (Guerzoni et al., 1997; Avila et al., 1998).

2.3.2. Smectite

The Guadalquivir River is considered as a main source of smectite and associated expandable minerals (Mélières, 1973; Auffret et al., 1974; López-Galindo et al., 1999; Machado, 2005; Alonso et al., 2016). The Guadalquivir Quaternary alluvial plain and present-day Bailen plain are enriched in smectite (up to 60 and 50%, respectively) resulting from the erosion of metamorphic and sedimentary rocks of the Betic range and of post-orogenic sedimentary formations (Mélières, 1973; Gutiérrez-Mas et al., 2006; Alonso et al., 2016). This high smectite content contrasts with the lower values observed in the nearby prodelta (Fernández-Caliani et al., 1997; López-Galindo et al., 1999; Gonzalez et al., 2004; Machado, 2005). Few studies evidence gravity-driven transfers of smectite perpendicularly to the isobaths. Smectite may locally be a significant component of sedimentation, representing up to 40% of the clay-fraction south of the Cadiz Bay, at the mouth of the Guadalete and Sanctipetri rivers which drain Miocene units of the Betic Cordilleras (López-Galindo et al., 1999; Machado, 2005; Achab et al., 2008). Some studies indicate that this smectite is deposited rapidly and is not further transported (Mélières, 1973; Palanques et al., 1995; Nelson and Maldonado, 1999).

By contrast, smectite is scarce in the Guadiana and the Tinto-Odiel rivers SPM (0–10%) and estuaries (Fernández-Caliani et al., 1997; Machado, 2005; Machado et al., 2007), reflecting the composition of pre-orogenic outcrops from the Iberian Massif (Gutiérrez-Mas et al., 2006; Alonso et al., 2016). Central Sahara dust, Western Mediterranean dust, and Moroccan dust are relatively depleted in smectite and are not considered as main sources of this clay mineral in the Gulf of Cadiz (Avila et al., 1997, 1998; Guerzoni et al., 1997). The Alboran Sea is mentioned as a potential source of smectite in the Gulf of Cadiz via the MOW (Pierce and Stanley, 1975; Grousset et al., 1988; Alonso et al., 2016). Hence, as a result of enhanced buoyancy which favors its long-range transport as suspended particles, smectite is particularly abundant in SPM of the Gulf of Cadiz (64%) and the Alboran Sea (67%) compared with their underlying sediments (5–25%) (Pierce and Stanley, 1975; Auffret et al., 1974; Grousset et al., 1988; Gutiérrez-Mas et al., 2003, 2006). The excess of smectite (up to 79% of the clay mineral fraction) in the SPM is especially observed in a near-bottom turbid layer in the Alboran Sea and in the Gulf of Cadiz, and coincides with the path of the MOW (Pierce and Stanley, 1975; Grousset et al., 1988).

2.3.3. Kaolinite

Kaolinite is a final product of hydrolysis processes and characterizes

highly-weathered environments (Chamley, 1989; Caquineau et al., 2002; Bout-Roumazeilles et al., 2013). As a result, kaolinite is particularly abundant in the Ebro River (30%) which drains kaolinite-rich continental deposits (Alonso and Maldonado, 1990) and in the Loukkos River (80%) (Palma et al., 2012). The Tinto-Odiel rivers and Guadiana River transport kaolinite (5–35%) toward the Gulf of Cadiz together with illite (Fernández-Caliani et al., 1997; Machado, 2005). Moroccan soils (38%) and the Algerian shelf (25%) are also potential contributors of kaolinite in the Gulf of Cadiz and Alboran Sea (Mélières, 1973; Elmouden et al., 2005).

The Guadalquivir, Guadalete and Sanctipetri rivers are not considered as major contributors of Kaolinite to the Gulf of Cadiz (Mélières, 1973; Gutiérrez-Mas et al., 2003, 2006; Achab et al., 2008). Kaolinite is not a major component of Alboran Sea sediments (15%) (Auffret et al., 1974; Grousset et al., 1988; Bout-Roumazeilles et al., 2007) whereas SPM from both the Alboran Sea and the Gulf of Cadiz may contain abundant kaolinite (Pierce and Stanley, 1975).

2.3.4. Illite/kaolinite ratio

The long-range conservative illite/kaolinite (I/K) ratio has been widely used to highlight differential settling processes (Machado, 2005) and to discriminate Saharian versus Sahelian sources in North African dust (Avila et al., 1997; Caquineau et al., 2002; Bout-Roumazeilles et al., 2007, 2013; Formenti et al., 2008; Kandler et al., 2009). This ratio efficiently distinguishes NW Saharan sources (I/K up to 11) from south and central Sahara (I/K = 0.4) and NE African and Sahelian sources (I/K = 0.1–0.2). Also, the I/K ratio which characterizes river-derived fine sediment displays an extensive range of values according to the river source: from 0 to 1 for Loukkos River (Palma et al., 2012), to 1–4 for the Guadalquivir River (Gutiérrez-Mas et al., 2003, 2006; Achab et al., 2008), 3–4 for the Tinto-Odiel and Guadiana rivers (Fernández-Caliani et al., 1997; Machado et al., 2007), and up to 6–8 in the Sanctipetri and Guadalete rivers (Gutiérrez-Mas et al., 2006; Achab et al., 2008).

3. Material and methods

3.1. Material

The study material was retrieved during Integrated Ocean Drilling Program (IODP) Expedition 339 (Stow et al., 2013a) in November 2011 to January 2012 and during the CADISAR cruise on RV *Le Suroît* in August 2001. IODP sites U1386, U1389 and U1390 were drilled on the Faro Drift (560 mbsl), the Huelva Drift (644 mbsl) and a large sheeted drift located southeast of the Guadalquivir Bank (992 mbsl), respectively (Fig. 1; Table 1). The continuous sedimentary records of these IODP sites, ranging from 6 m composite depth (mcd) to 22 mcd, allow to reconstruct clay mineral variations in three distinct drifts over the last 25 kyrs.

In addition, thirteen piston cores from the CADISAR cruise (Table 1; Fig. 1B) were used to achieve a complete record of clay deposition. These cores, principally located under the influence of MOW_L, are sampled in a range of sedimentary bodies over channel/ridge and overflow sedimentary lobe sectors encompassing the Guadalquivir Channel (738–757 mbsl), Guadalquivir Bank (737–786 mbsl), a giant contouritic levee (814 mbsl) and the sector below the Guadalquivir Ridge (813–1001 mbsl). Two of the piston cores from the CADISAR cruise, CADKS24 (1316 mbsl) and CADKS25, were collected in the lower slope, at the limit of MOW_L influence (Fig. 1A).

Table 1
Details of IODP sites and piston cores used in this study.

Cores/sites/depth (m)	Latitude	Longitude	Depositional setting	Water masses on the seafloor (at the present time)
U1386 (560)	36.83	−7.76	Faro Drift	MOW_U
U1389 (644)	36.43	−7.28	Huelva Drift	MOW proximal
CADKS11 (757)	36.40	−7.48	Guadalquivir Channel	
CADKS12 (746)	36.41	−7.48		
CADKS13 (750)	36.42	−7.49		
CADKS14 (738)	36.42	−7.52		
CADKS22 (786)	36.42	−7.95	Guadalquivir Bank	
CADKS23 (737)	36.44	−7.92		
CADKS04 (814)	35.88	−6.93	Giant contouritic levee	MOW_L
CADKS16 (813)	36.33	−7.39	South Guadalquivir ridge	
CADKS17 (852)	36.33	−7.38		
CADKS18 (1001)	36.30	−7.41		
U1390 (992)	36.32	−7.72	Large sheeted drift southeast of the Guadalquivir Bank	
CADKS21 (1008)	36.21	−7.76	Guadalquivir Drift	
CADKS24 (1316)	36.08	−7.94	Lower slope	Limit of influence of MOW_L
CADKS25 (1256)	36.15	−8.00	Lolita mud volcano	

3.2. Age models

3.2.1. IODP sites

The stratigraphy of IODP Site U1386 for the last 25 kyrs cal. BP is constrained by five AMS^{14}C ages and by one correlation point to LR04 (Kaboth et al., 2016). Chronology of IODP Site U1389 is based on a combination of AMS^{14}C dating and visual correlations of planktonic $\delta^{18}O$ records with North Greenland Ice Core Project (NGRIP) and the Iberian margin core MD01-2444 (Bahr et al., 2015). The age model of IODP Site U1390 combines AMS^{14}C dates and tie points based on visual correlation between planktonic $\delta^{18}O$ records and NGRIP (van Dijk et al., 2018). The sedimentation rates obtained in this study at IODP sites U1386, U1389 and U1390 range between 0.16 m kyrs^{-1} (Site U1386) and 3.46 m kyrs^{-1} (Site U1390) for the last 25 kyrs.

3.2.2. CADISAR cores

The chronostratigraphy of the thirteen CADISAR cores used in this study is constrained by a biostratigraphic framework based on planktonic foraminiferal abundances, as proposed by Ducassou et al. (2018). Faunal analyses of Hassan (2014) and Ducassou et al. (2018) allow the identification of several bio-events, including Heinrich Stadial 2 (HS2), Heinrich Stadial 1 (HS1) and *Globorotalia truncatulinoides* sinistral events (TE2). In this study, the interval between HS2 (23,800–24,500 years cal. BP) and HS1 (15,350–17,950 years cal. BP) bio-events, which are both characterized by a peak in the relative contribution of *Neogloboquadrina pachyderma* (>10%) to the bulk planktonic foraminiferal assemblages (Ducassou et al., 2018), is used to constrain the Last Glacial Maximum. The second most recent peak abundance of *G. truncatulinoides* sinistral, named TE2 which occurs between 3250 and 4250 years cal. BP (Ducassou et al., 2018), allows us to pinpoint the Late Holocene deposition.

3.3. Methods

3.3.1. Clay mineralogy

Following a protocol adapted from Bout-Roumazeilles et al. (1999) the carbonate-free fraction, obtained using 0.1 N hydrochloric acid, is deflocculated by repeated washes with distilled water. The clay-size

fraction (<2 μm) is isolated by settling following the approximation of Stoke'Law, and concentrated by centrifugation (40 min at 3500 rpm), before orienting the aliquot on glass slides. Three X-ray diffraction (XRD) runs—air-dried sample, ethylene-glycol saturation for 24 h in high vacuum, and heated sample (490 °C for 2 h)—are performed using a Bruker D4 Endeavour (Cu kα, Ni filter) coupled with a Lynxeye rapid detector between 2.5°2θ and 32.5°2θ.

Semi-quantitative estimation of the main clay minerals is based on their reticular (basal + interlayer) distance on the XRD spectra, according to their main respective crystallographic structures (Brown, 1980). Smectite (S) is characterized by a main peak between 14 and 15 Å on the air-dried test that expands at 17 Å after ethylene-glycol saturation and retracts down at 10 Å after heating. Illite (I) is represented by basal peaks at 10 Å, 5 Å and 3.33 Å on the three tests. Chlorite (C) is identified by peaks at 14.2 Å, 7.1 Å, 4.75 Å and 3.54 Å on the three tests. Kaolinite (K) is determined by peaks at 7.2 Å and 3.58 Å that disappear or are strongly reduced after heating.

Semi-quantitative estimation of the clay mineral fraction is based on peak areas - 17 Å for smectite, 10 Å for illite and 7.1–7.2 Å for chlorite+kaolinite- as measured on the ethylene glycol saturation spectra summed at 100% using the Macdiff 4.2.5 software (Petschick, 2000) Distinction between kaolinite and chlorite is based on a pseudo-voigt deconvolution for the K-C doublet (3.58 Å–3.54 Å) (Petschick, 2002).

In order to prevent any bias or misinterpretation due to the comparison of our dataset with previously published data—some of which are obtained using different analytical protocols or routines (using weighted correction factors) —we compare clay-mineral ratios (I/K, S/K and C/K) rather than percentages (Bout-Roumazeilles et al., 2013). Moreover, illite-smectite mixed-layers reported in some previously published or unpublished dataset are included in the smectite percentages for further comparison with our own dataset.

3.3.2. Grain-size analyses

Grain-size analyses are performed on the bulk sediment of IODP Sites U1386 and U1390 using a Malvern MASTERSIZER S (University of Bordeaux, UMR 5805 EPOC). Coaser intervals are sampled at a 4–5 cm resolution, while homogeneous muddy layers are analised every 24–32 cm. The mean size of sortable silt is used as index of bottom flow speed (McCave et al., 1995), and the percentage of particles <10 μm is used to represent clay particle amount in sediment. The difference between the percentage of bulk particles <10 μm and carbonate-free particles <10 μm generally does not exceed 10% except in the coarsest facies of contourite sequences where it reaches 18%. This weak discrepancy is also observed during the Holocene when coccolith abundance was especially high in sediments of the upper slope and the lower slope of the Gulf of Cadiz (Sierro et al., 1999; Colmenero-Hidalgo et al., 2004). We therefore infer that coccolith abundances have little influence on the percentage of particles <10 μm which can be thus used as indicator of clay particle amount.

4. Results

4.1. Sub-actual spatial distribution of clay minerals in the Gulf of Cadiz

The clay mineral fraction displays important variations depending of the location of the cores and their environmental settings (Table 2; Fig. 1). The percentages of smectite range between 19% and 54% showing large variations in sub-surface sediments of the middle slope of the Gulf of Cadiz (Table 2). The relative abundance of smectite is generally high in sediments of the Faro Drift (45%) and the south Guadalquivir Ridge (38–54%; Fig. 2; Table 2). Smectite is also a major component of clay mineral assemblages in the surface sediments of the Huelva (34%) and Guadalquivir Drifts (36%; Fig. 2; Table 2). In contrast, sediments in the large sheeted Drift southeast of theGuadalquivir Bank (19%) and the giant contouritic levee (26%) are characterized by smectite values two to three times lower than those in sediment bodies

Table 2
Clay mineral relative abundances in sub-surface samples from IODP sites (±5%) and CADISAR cores.

Cores/sites/ depth (mbsl)	Sample depth (cm)	% S	%I	% C	% K	Depositional setting
U1386 (560)	***8***	***45***	***34***	***16***	***5***	Faro Drift
U1389 (644)	***6***	***34***	***34***	***12***	***20***	Huelva Drift
CADKS11 (757)	***4***	***51***	***24***	***15***	***10***	
CADKS12 (746)	***4***	***32***	***33***	***19***	***16***	
CADKS13 (750)	***2***	***43***	***27***	***14***	***16***	Guadalquivir Channel
CADKS14 (738)	***4***	***30***	***35***	***16***	***18***	
CADKS22 (786)	***2***	***32***	***33***	***17***	***18***	
CADKS23 (737)	***3***	***31***	***33***	***13***	***23***	Guadalquivir Bank
CADKS04 (814)	***4***	***26***	***34***	***18***	***23***	Giant contouritic levee
CADKS16 (813)	***4***	***45***	***24***	***11***	***20***	
CADKS17 (852)	***6***	***54***	***22***	***10***	***14***	Below Guadalquivir Ridge
CADKS18 (1001)	***3***	***38***	***27***	***15***	***20***	
U1390 (992)	***18***	***19***	***44***	***14***	***24***	Southeast of the Guadalquivir Bank a large sheeted drift
CADKS21 (1008)	***2***	***36***	***29***	***13***	***22***	Guadalquivir Drift
CADKS24 (1316)	***2***	***29***	***33***	***15***	***23***	Lower slope
CADKS25 (1256)	***4***	***34***	***32***	***13***	***21***	Lolita mud volcano

S: smectite; I: illite; C: chlorite; K: kaolinite.

mentioned above (Fig. 2; Table 2). CADISAR cores located on the lower slope contain surface sediments with intermediate smectite values (29–34%; Fig. 2; Table 2). The Guadalquivir Channel, dominated by erosive features, shows an important variability of smectite abundances (30–51%; Fig. 2; Table 2).

Illite varies between 22% and 44% but most sub-surface samples range between 32% and 35% (Table 2). Indeed, the illite content in surface sendiments of the Faro Drift, Huelva Drift, Guadalquivir Bank and Giant contouritic levee ranges between 33 and 34% (Fig. 2; Table 2), which reflects a homogenous distribution of this clay mineral into the sediment bodies of the upper part of Cadiz CDS (<~800 mbsl) except for the Guadalquivir Channel which displays a wide range of illite content (24–35%; Fig. 2; Table 2). The distribution of illite along the lower part of the CDS (> ~ 800 mbsl) is much more heterogenous. Illite content predominates (44%) in the large sheeted drift drilled by IODP Expedition 339 (Site U1390) whereas this clay mineral is less abundant in the south Guadalquivir Ridge (22–27%; Fig. 2; Table 2) and Guadalquivir Drift (29%; Table 2). Surface samples collected from the lower slope, on the edge of the CDS, are characterized by intermediate percentages of illite (32–33%, Fig. 2; Table 2).

Kaolinite and chlorite are less abundant than illite and smectite in the surface sediments of the middle slope of the Gulf of Cadiz. Kaolinite represents 5–24% of the total clay mineral fraction (Table 2). Surface sediments in the large sheeted drift southeast of the Guadalquivir Bank (24%), the Guadalquivir Drift (22%), located on the deep part of the middle slope (< ~1000 mbsl), and the lower slope (21–23%) display high kaolinite contents in (Fig. 2; Table 2). Kaolinite is also relatively abundant in surface samples from the Giant contouritic levee (23%), the Guadalquivir Bank (18–23%) and the Huelva Drift (20%), located in the upper part of the middle slope (> ~ 800 m; Fig. 2; Table 2). Surface sediments from the Guadalquivir Channel and from below Guadalquivir

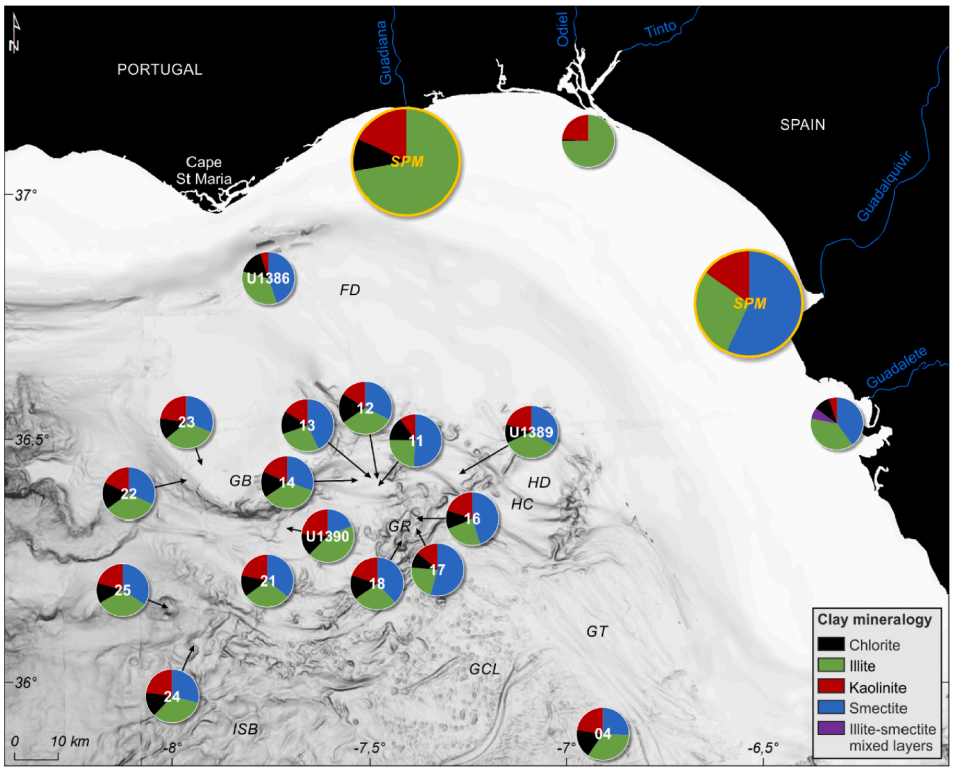

Fig. 2. Clay mineral composition of SPM in the Guadiana and Guadalquivir estuaries and in sediments from the Tinto-Odiel and Guadalete rivers mouths (Mélières, 1973; Fernández-Caliani et al., 1997; López-Galindo et al., 1999; Gutiérrez-Mas et al., 2006; Machado et al., 2007; Achab et al., 2008). Sub-surface clay mineral abundances in the middle slope of the Gulf of Cadiz (this study). SPM: Suspended Particulate Matter; FD: Faro Drift; HD: Huelva Drift; HC: Huelva Channel; GB: Guadalquivir Bank; GCL: Giant contouritic levee; GR: Guadalquivir Ridge; GT: Giant terrace; ISB: intraslope basin.

Ridge have variable kaolinite content (10–20%; Fig. 2; Table 2). Kaolinite contents in surface sediments from the Faro Drift (5%) are two to five times lower than values from the other surface samples from the CDS (Fig. 2; Table 2). Chlorite shows the lowest variability (10–19%) of all the clay minerals in the surface sediments of the middle slope of the Gulf of Cadiz (Fig. 2; Table 2). Surface sediments from the lower slope, Guadalquivir Drift and sheeted drift located southeast of the Guadalquivir Bank (the deepest part of the CDS) are characterized by chlorite contents centered around 14% (Fig. 2; Table 2). Surface sediments from the Guadalquivir Channel, the area below Guadalquivir Ridge and Bank, the Huelva Drift and the Faro Drift show a kaolinite contents rangig 10–19% (Fig. 2; Table 2).

4.2. *Temporal variations of clay mineral over the last 25 kyrs in the Gulf of Cadiz*

In order to reconstruct variations in clay mineral assemblages over the last 25 kyrs, we focuse on the high resolution IODP records. In addition, the sedimentary records from the CADISAR cruise are used to get a more global view of clay mineral deposition in the Gulf of Cadiz during specific time intervals of the LGM (18–25 kyrs cal. BP) and Late Holocene (last 5 kyrs cal. BP). However, due to the low sampling resolution, varying sedimentation rates and accuracy of the biostratigraphic age models (Hassan, 2014; Ducassou et al., 2018), it was not possible to determine the clay mineral association for the above-mentioned time intervals in all CADISAR cores.

The high resolution measurements at IODP sites enables us to analyse the significant variations of clay assemblages in the Faro drift, the Huelva drift and the large sheeted drift southwest of the Guadalquivir bank during the last 25 kyrs. During this time interval, the clay mineral association of Site U1386 comprises on average, in decreasing abundances, smectite (46%), illite (32%), chlorite (17%) and kaolinite (5%; Fig. 3), showing few differences with Site U1389 which is composed of smectite (44%), illite (29%), kaolinite (14%) and chlorite (12%; Fig. 4). Clay mineral assemblages at Site U1390 for the last 25 kyrs consist of illite (37%), smectite (29%), kaolinite (17%) and chlorite (17%; Fig. 5).

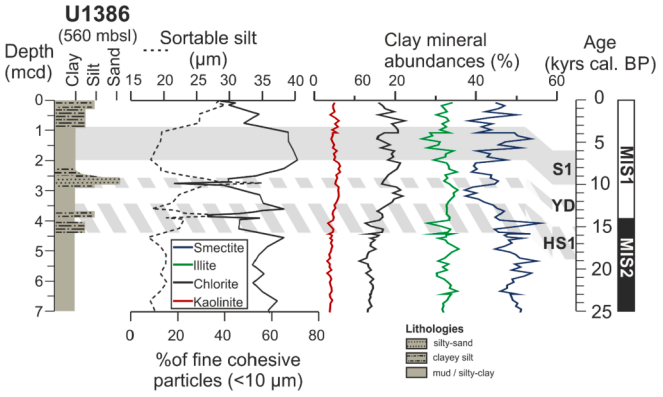

Fig. 3. Lithology, fine cohesive particle abundance (<10 μm), sortable silt (dashed line) and clay mineral variations in sediments from the Faro Drift (IODP Site U1386) for the last 25 kyrs. MIS: Marine Isotope Stage; HS1: Heinrich Stadial 1; YD: Younger Dryas; S1: Sapropel 1.

The LGM is characterized by high average percentages of smectite at sites U1386 (50%), U1389 (47%) and U1390 (31%; Table 3). During this period, smectite contents at the IODP sites display a sequence of consecutive brief increases and decreases, with maximum smectite abundance during HS1 (Figs. 3 to 5). Smectite contents then drop significantly during the end of HS1 from 56% down to 37% for IODP Site U1386, from 59% down to 17% for IODP Site U1389, and from 38% down to 20% for IODP Site U1390 (Figs. 3 to 5). The Younger Dryas is characterized by a peak of smectite percentages at IODP sites U1389 (55%) and U1390 (36%; Figs. 4 and 5). From the Younger Dryas to the Late Holocene, sediments from IODP Site U1390 shift gradually between high and low smectite contents (Fig. 5). IODP Site U1389 shows an increasing trend of smectite content despite relatively large oscillations, while IODP Site U1386 displays rapid changes in smectite content with high values during the period of Sapropel 1 deposition (54%; Fig. 3).

Illite contents at IODP sites U1386 (27–36%) and U1389 (22–38%)

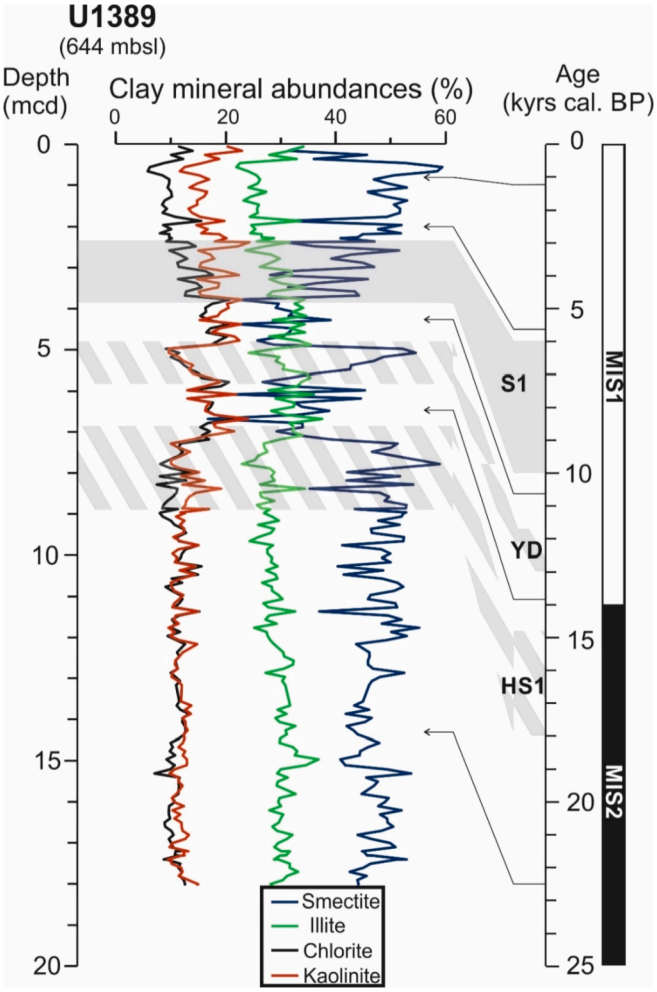

Fig. 4. Clay mineral variations in the Huelva Drift (IODP Site U1389) for the last 25 kyrs. The black arrows correspond to AMS^{14}C ages from Bahr et al. (2015). MIS: Marine Isotope Stage; HS1: Heinrich Stadial 1; YD: Younger Dryas; S1: Sapropel 1.

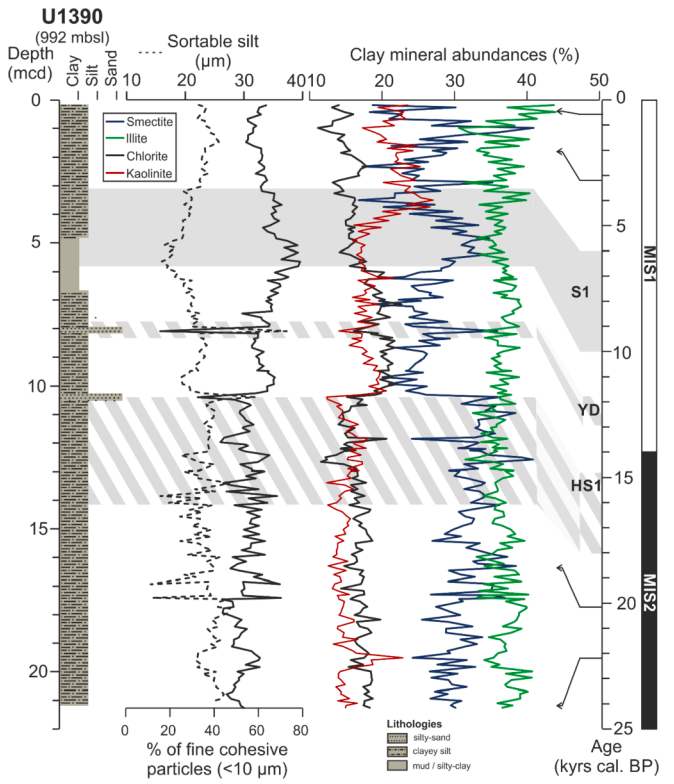

Fig. 5. Lithology, fine cohesive particle abundance (<10 μm), sortable silt (dashed line and clay mineral variations in sediments from the large sheeted drift southeast of the Guadalquivir Bank (IODP Site U1390) for the last 22 kyrs. The black arrows correspond to AMS^{14}C ages from van Dijk et al. (2018). MIS: Marine Isotope Stage; HS1: Heinrich Stadial 1; YD: Younger Dryas; S1: Sapropel 1.

vary over the last 25 kyrs (Figs. 3 and 4). Sediments from the Faro drift do not display any specific trend in illite abundances during this period (Fig. 3), but illite content in the Huelva drift shows two significant increases toward the end of HS1 and during the Late Holocene (Fig. 4). The abundance of illite, the dominat clay mineral at IODP Site U1390 over the last 25 kyrs (31–44%), shows many relatively quick changes with maximum values toward the end of the Late Holocene (Fig. 5).

Kaolinite and chlorite are less abundant at IODP Sites U1386 (5–22%), U1389 (6–24%), and U1390 (11–27%; Figs. 3–5). The Faro drift is distinguished by its low smectite content (≤5%) and by a gradual increase of approximately 8% in the chlorite content from HS1 to the beginning of YD (Fig. 3). Kaolinite and chlorite percentages at the Huelva drift and large sheeted drift southwest Guadalquivir bank are relatively similar until the period of Sapropel 1 deposition (Figs. 4 and 5). IODP Site 1389 is characterized by three increases of kaolinite and chlorite content during the end of (1) HS1 (>12%), (2) duringYounger Dryas (>11%), and (3) during Late Holocene (>8%; Fig. 4). IODP Site 1389 also shows a rise of more than 8% in kaolinite and chlorite abundances during the end of HS1 (Fig. 5). Kaolinite content increases from 16% to 27% during the period of Sapropel 1 deposition, whereas the illite content remains constant (Fig. 5).

CADISAR cores CADKS23 and CADKS04, as well as IODP sites U1386 and U1390, are characterized by a slightly higher average smectite content (4–5% greater) during the LGM than during the Late Holocene (Table 3). The smectite contents in cores CADKS24 and CADKS25, as well as at IODP Site U1389 remain relatively stable, or increase slightly during both these periods (Table 3). Illite contents in the CADISAR cores and at IODP sites does not vary significantly between the LGM and the Late Holocene, except at IODP Site U1390 where illite percentages decreases from 30 to 26% (Table 3). Almost all CADISAR cores and IODP sites mentioned above are characterized by lower average chlorite contents during the Late Holocene than during LGM with a more marked drop (5–6% greater) for the cores located on the lower slope (CADSKS24 and CADKS25; Table 3). In contrast, sediments from the Giant

Table 3
Comparison of average clay mineral contents in cores CADKS04, CADKS23, CADKS24 and CADKS25 and IODP sites U1386, U1389 and U1390, during the Late Holocene (<5 kyrs cal. BP) and during the Last Glacial Maximum (18–25 kyrs cal. BP).

Cores (depth mbsl)	Core samples (cm)	% S	% I	% C	% K	Depositional setting
CADKS04	4–40	25	34	18	24	Giant contouritic levee
(814)	160–240	29	35	20	16	
CADKS23	3	31	33	13	23	Guadalquivir Bank
(737)	69–80	36	32	15	17	
CADKS24	2	29	33	15	23	Lower slope
(1316)	535–795	30	33	20	17	
CADKS25	4	34	32	13	21	Lolita mud volcano (lower slope)
(1256)	334–689	32	33	19	17	
IODP U1386	8–68	45	32	18	5	Faro drift
(560)	408–574	50	32	14	4	
IODP U1389	9–176	48	26	10	16	Huelva drift
(664)	896–1561	47	30	11	12	
IODP U1390	18–232	27	37	15	22	Sheeted drift
(992)	1432–2125	31	37	17	15	

contouritic levee, Guadalquivir bank, Faro drift, Huelva drift, large sheeted drift southeast of the Guadalquivir bank and the lower slope contain higher kaolinite values during Late Holocene than during the LGM (4–7% greater; Table 3).

The percentage of fine cohesive particles (<10 μm) varies between 15% and 79% over the last 25 kyrs at sites U1386 and U1390 (Figs. 3 and 5). The proportion of clay particles is negatively correlated with sortable silt values which is commonly used as an indicator of MOW velocity in the Gulf of Cadiz (Toucanne et al., 2007). This clearly reveals the dominant role of the MOW on fine-grained particle deposition/winnowing in these drifts. This is illustrated by the low contents in cohesive particles which are associated with coarse layers at IODP Sites U1386 and U1390 during HS1 and YD (Figs. 3 and 5). These intervals are described as contourite peaks I and II (Faugères et al., 1986) and indicate strengthening of the speed of the MOW (e.g., Faugères et al., 1984; Gonthier et al., 1984; Stow et al., 1986). A similar decrease in fine cohesive particles is observed at Site U1386 during the contourite peak III, which characterizes the end of the Holocene (Faugères et al., 1986). Furthermore, the <10 μm fraction maximum during Sapropel 1 deposition confirms furthermore the major influence of MOW velocity on fine cohesive particle deposition (Fig. 5).

5. Discussion

5.1. Clay transport: from river discharge and eolian input to deposition in the middle slope of the Gulf of Cadiz

The potential sources of clay minerals in the middle slope of the Gulf of Cadiz can be clustered into the following three endmembers, the possibility of diagenetic clays having been discarded as samples are from very shallow sub-surface:

(I) the northwest African endmember, mainly composed of western Mediterranean eolian dust (Guerzoni et al., 1997), Northwestern African dust and soils (Grousset et al., 1992; Elmouden et al., 2005) and Morroccan river assemblages (Snoussi, 1986), and characterized by high kaolinite + chlorite and low smectite contents (Fig. 6).

(II) the eastern endmember of Gulf of Cadiz comprises assemblages from the Guadalquivir and Guadalete Rivers, both particularly enriched in smectite (Mélières, 1973; Gutiérrez-Mas et al., 2006)

(III) the illite-rich north pole of Gulf of Cadiz endmember including assemblages from the Guadiana and Tinto-Odiel rivers as well as the more distant Tagus River (Lima, 1971; Fernández-Caliani et al., 1997; Machado et al., 2007).

Most samples analysed in this study plot between two African pole (I) and the Gulf of Cadiz east pole (II) (Fig. 6), evidencing that clay particles deposited in the CDS of the Gulf of Cadiz mostly result from a mix between these two clusters. The clay mineral composition of the "Gulf of Cadiz north pole" sources differs strongly from assemblages of IODP Sites and CADISAR cores (Fig. 6), suggesting that this pole has a limited contribution to sedimentation in the CDS. For example, the nearby smectite-rich Faro Drift sediments contrast significantly with the illite-rich and smectite-depleted clay mineral composition of Guadiana Estuary (Fig. 6; Machado et al., 2007). The Guadiana River is nevertheless considered as one of the main sediment supplier to the adjacent margins with an estimated sediment supply of $2.9*10^6$ t yr^{-1} (Machado et al., 2007). The weak contribution of detrital discharge from northern rivers to clay particle sedimentation on the slope is primarily related to the preferential deposition of clay minerals from the Guadiana and Tinto-Odiel rivers on the shelf. These proximally deposited clays form the Guadiana Mud Patch (Gonzalez et al., 2004; Rosa et al., 2011). The surface and deep circulation patterns may also play an important role on both redistribution and settling of terrigenous particles. Cyclonic eddies located on the northern continental shelf of the Gulf of Cadiz probably act as a sediment trap, preventing export of fine particles to the middle slope (Fig. 1). Moreover, the MOW_U, which circulates along the continental slope, forms an effective barrier against offshore clay particle export between the Guadiana and Tinto-Odiel Estuaries and the Faro Drift. Alonso et al. (2016) demonstrated that the Faro Drift was occasionally supplied by illite-rich (>73%) gravity-flows carrying fine particles from Guadiana and Tinto-Odiel Rivers.

The significant proportion of smectite in fine sediments from the Gulf of Cadiz (Fig. 6) suggests that rivers located east of the Gulf of Cadiz and particularly the Guadalquivir River, with its important discharge ($5.9*10^6$ t yr^{-1}), are an important source of clay particles in the CDS as proposed by Grousset et al. (1988) and Alonso et al. (2016). Indeed, the Guadalquivir River mouth SPM is characterized by particularly high smectite content (~57%)(Fig. 2; Mélières, 1974). The southeastern continental margin of the Gulf of Cadiz is nevertheless depleted in smectite which is far less abundant than illite in surface sediments (López-Galindo et al., 1999; Machado, 2005; Gutiérrez-Mas et al., 2006;

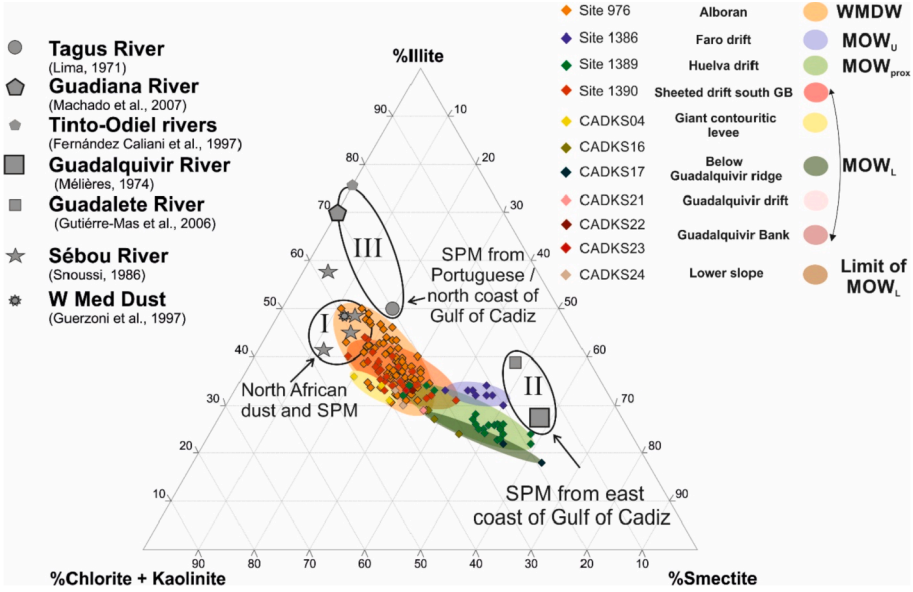

Fig. 6. Smectite vs. illite vs. chlorite + kaolinite ternary plot for samples covering the last 5 kyrs from this study and the Alboran Sea (Bout-Roumazeilles et al., 2007). Endmembers are derived from previous published records and divided into three groups: North African dust and Suspended Particle Matter (SPM; I), SPM from the eastern pole of the Gulf of Cadiz (II) and SPM from the northern pole of the Gulf of Cadiz (III). WMDW: Western Mediterranean Deep Water; MOW: Mediterranean Outflow Water; MOW_U: upper branch of the MOW; MOW_{PROX}: proximal MOW; MOW_L: lower branch of the MOW.

Achab et al., 2008). This observation suggests specific differential transport or winnowing of smectite-rich river-borne particles by surface currents. Indeed smectite-rich particles from the Guadalquivir River are thought to be transported through the Strait of Gibraltar by the Atlantic Inflow, thereby allowing a west-to-east enrichment in smectite in the Alboran Sea (Auffret et al., 1974; Pierce and Stanley, 1975; Grousset et al., 1988; Vergnaud-Grazzini et al., 1989; López-Galindo et al., 1999). Thereafter, suspended fine particles are partly redirected westward by the MOW at intermediate depths and feed the middle slope of the Gulf of Cadiz (Grousset et al., 1988; Vergnaud-Grazzini et al., 1989; López-Galindo et al., 1999), explaining the unexpected smectite content in the CDS compared with the smectite-depleted sedimentation observed on the Gulf of Cadiz southeastern continental margin. Moreover, some authors used the smectite content as an efficient MOW tracer beyond the Gulf of Cadiz in the Western Portuguese margins (Grousset et al., 1988; Vergnaud-Grazzini et al., 1989; Schönfeld, 1997; Stumpf et al., 2011).

The high chlorite + kaolinite and low smectite content observed in some samples from IODP sites and CADISAR cores implies the contribution of another source of clay particles together with the previously identified Gulf of Cadiz smectite-rich eastern endmember (II; Fig. 6). The similarity between clay mineral assemblages in rivers, soils and dusts from northwestern Africa (Snoussi, 1986; Grousset et al., 1992; Guerzoni et al., 1997; Elmouden et al., 2005), sediments from the Alboran Sea (Bout-Roumazeilles et al., 2007) and some of our CDS sediments suggests that the northwest African pole as a significant source. Grousset et al. (1988) and Stumpf et al. (2011) have both underlined the existence of this "African" Endmember, based on isotope analyses. However, Grousset et al. (1988) also proposed that kaolinite might be supplied via the Guadalquivir River, since smectite and kaolinite display rather similar distributions. As we do not observe any similar pattern between smectite and kaolinite deposition in the studied samples (Figs. 3, 4 and 5), we propose that kaolinite has a primary Northwestern African origin, in line with Stumpf et al. (2011).

The C/K ratio was used in order to pinpoint the influence of kaolinite-rich supply from the Northwest African pole into the Gulf of Cadiz and Alboran Sea (Fig. 7). Comparable C/K ratios at IODP Sites U1389 and U1390 reflect similar terrigenous sources, despite the fact that these IODP sites are located under the respective influence of the proximal MOW (MOW_{PROX}) and the lower MOW (MOW_L). Moreover, the close correspondence between the C/K ratios of IODP sites 1389 and U1390 the ODP Site 976 in the Alboran Sea, strongly suggests that northwest African Material is initially deposited in the Alboran Sea before being redistributed by the MOW toward the CDS of the Gulf of Cadiz (Fig. 7). The strong discrepancy between C/K ratios at IODP Site U1386, and IODP Sites U1389 and U1390 reflect different terrigenous fine-grained sourcing over the CDS of Gulf of Cadiz (Fig. 7).

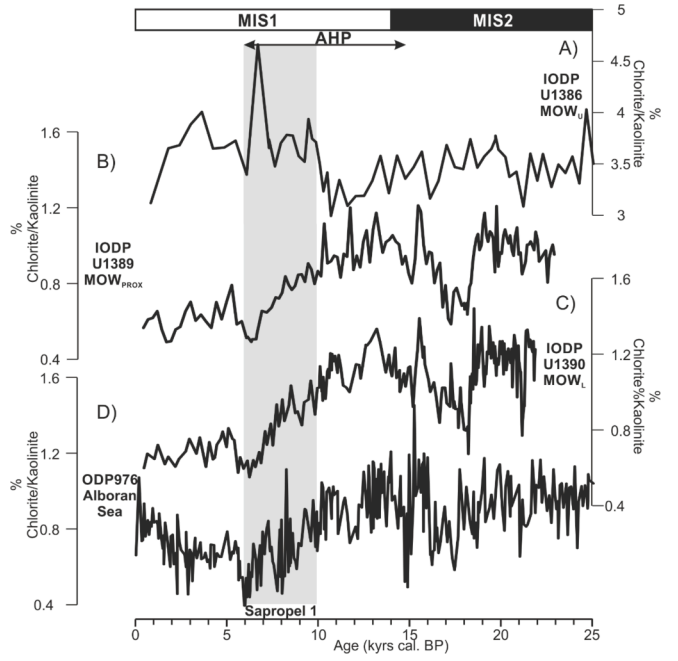

Fig. 7. Chlorite/Kaolinite ratio over the last 25 kyrs at IODP sites influenced by (A) the upper core of the MOW (MOW_U), (B) the proximal MOW (MOW_{PROX}), (C) the lower core of the MOW (MOW_L) and (D) ODP Site in the Alboran Sea (Bout-Roumazeilles et al., 2007). MIS: Marine Isotope Stage; AHP: African Humid Period.

5.2. MOW pathway and fine particle deposition in drifts of the Gulf of Cadiz

In order to understand and to focus on the depositional pattern of clay particles transported by the MOW and thus to limit the influence of downslope processes, forthcoming interpretations are only based on data from sedimentary drifts. Sediment deposition on large drifts in the Gulf of Cadiz is widely dominated by along-slope processes (Faugères et al., 1984; Stow et al., 1986; Mulder et al., 2002; Habgood et al., 2003; Hernández-Molina et al., 2003, 2006; Hanquiez et al., 2007; Llave et al., 2007; García et al., 2009; Roque et al., 2012; Bankole et al., 2020) allowing the accumulation of principally fine-grained sediments (Faugères et al., 1984; Gonthier et al., 1984; Stow et al., 1986; Lofi et al., 2016; De Castro et al., 2020, 2021). Recent studies indicate that downslope processes have sporadically influenced the Huelva Drift during its formation(Bankole et al., 2020; De Castro et al., 2020, 2021)–. However, recent studies which investigated the sedimentary records of IODP Sites U1386, U1389 and U1390 over the last 25 kyrs cal. BP, have not observed any evidences of turbidity current effects on sedimentation at these IODP sites (Bahr et al., 2015; Kaboth et al., 2017; van Dijk et al., 2018).

Bottom waters, by combining advection and resuspension, are often characterized by nepheloid layers with a high SPM content (Biscaye and Eittreim, 1977; McCave, 1986). Several studies have documented the high SPM concentrations of the MOW in the Gulf of Cadiz with values between 0.03 and 0.94 mg/l (Pierce and Stanley, 1975; Ambar et al., 2002; Freitas and Abrantes, 2002) without any significant difference between MOW_U and MOW_L in terms of concentration and composition of SPM (Freitas and Abrantes, 2002). The Faro Drift (U1386) and the large-sheeted drift south of the Guadalquivir Bank of the CDS (U1390) exhibit similar percentages of fine-grained sediments (<10 μm) that culminate during the Sapropel 1 deposition (72–78%) while reaching minimum values (15–18%) during the Younger Dryas (Fig. 8). However, IODP Site U1390 located under the path of the MOW_L, is characterized by sedimentation rates between two and ten times higher than MOW_U influenced IODP Site U1386 (Fig. 8; van Dijk et al., 2018). Huelva Drift sedimentation rates (IODP Site U1389; MOW_{PROX}) are similar to those observed at Faro Drift during MIS1 (0.23–0.69 m $kyrs^{-1}$) with a significant increase (>1 m $kyrs^{-1}$) during the MIS2 (Bahr et al., 2015; Fig. 8). Various factors may explain strong discrepancies in sedimentation rates between these drifts despite a rather homogenous percentage of fine cohesive particles. Topographic irregularities control MOW pathways in the middle slope of the Gulf of Cadiz and therefore play a critical role in CDS sedimentation (e.g., Madelain, 1970; Hernández-Molina et al., 2006). The distance of these different IODP sites from the main cores of MOW_U and MOW_L may also play a crucial role in sediment deposition on drifts, and may explain the difference in sedimentation rates between them. Sedimentation rate changes, such as the synchronous increase at IODP sites U1389 and U1390 during MIS2 (Fig. 8), may reflect vertical shifts in the cores of the MOW, thus increasing the deposition of sediment. It has also been suggested that the current similar overall concentrations and compositions of SPM in MOW_U and MOW_L (Freitas and Abrantes, 2002) may not hold for the last 25 kyrs. In particular, varying SPM concentrations in MOW_U and MOW_L at the beginning of Holocene and during MIS2, may explain contrasted

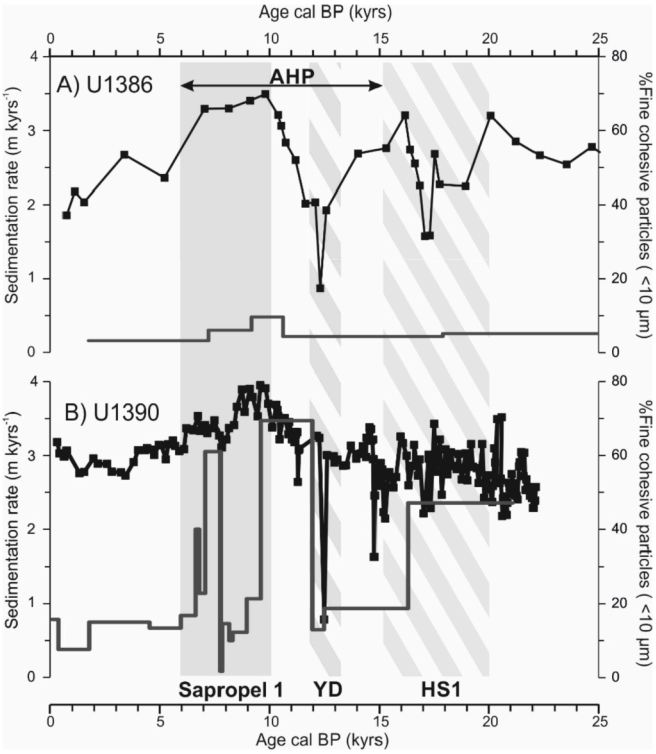

Fig. 8. Sedimentation rates (dark grey line) and % of fine cohesive particles (<10 µm; black squares and line) of IODP sites U1386 (A) and U1390 (B) for the last 25 kyrs cal. BP. AHP: African Humid Period; HS: Heinrich Stadial; YD: Younger Dryas.

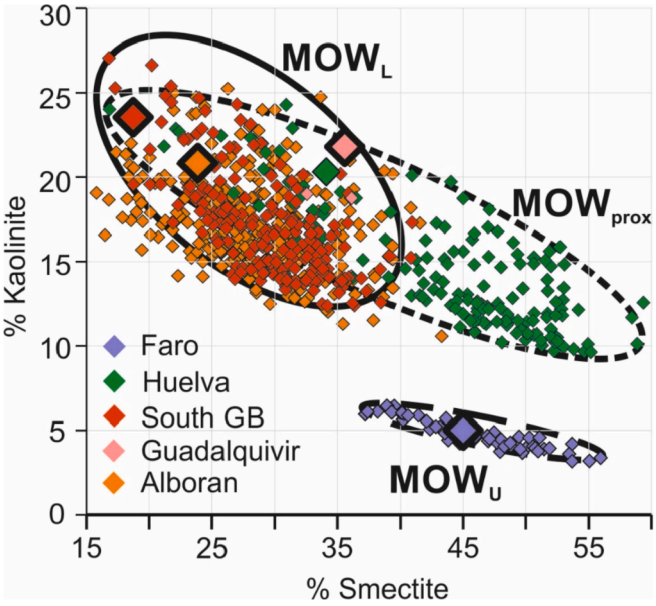

Fig. 9. Binary kaolinite vs. smectite plot fro the clay mineralogy in the Faro Drift (IODP Site U1386), Huelva Drift (IODP Site U1389), large sheeted drift south of the Guadalquivir Bank (IODP Site U1390), Guadalquivir Drift (core CADKS21) and Alboran Sea (ODP Site 976; Bout-Roumazeilles et al., 2007) over the last 25 kyrs cal. BP. These drifts are influenced by MOW_U, MOW_L and both MOW_{PROX}. Large rhombs represent sub-surface samples.

sedimentation rates (respectively four and ten times higher) observed in the sheeted drift southeast of the Guadalquivir Bank (U1390) compared with the Faro Drift (U1386; Fig. 8).

5.3. Clay mineral deposition mechanisms along the path of the MOW

The clay mineral compositions of four drift deposits (U1386, U1389, U1390 and CADKS21), located at different depths along the middle slope of the Gulf of Cadiz, displays a general trend, in particular regarding kaolinite and smectite deposition. Kaolinite relative abundance appears to be two to five times higher in IODP sites U1389 and U1390 (Huelva Drift and southeast of the Guadalquivir Bank sheeted drift, respectively) and CADKS21 core (Guadalquivir Drift) located under the path of proximal and lower MOW (10–27%) than at IODP Site U1386 (Faro Drift) located under the path of MOW_U (3–6%) which appears largely depleted in kaolinite (Fig. 9). By contrast, smectite abundances range from 37 to 56% in the Faro Drift under the MOW_U, while ranging between 17% and 41% at the drifts (U1390 and CADKS21) influenced by MOW_L (Fig. 9). IODP Site U1389, which is influenced by both MOW_L and MOW_U, displays a wide range of smectite concentrations (17–63%; Fig. 9). Four main mechanisms can be invoked to explain lateral differential distribution of clay minerals: differential settlling, particle aggregation, authigenisis, and clay mineral sorting (e.g., Chamley, 1989).

The relationship between differential settling of clays and fine particle flocculation depends on various parameter changes such as water density, temperature, salinity, as evidenced in laboratory experiments (e.g., Whitehouse et al., 1960; Chamley, 1989) and as supported by studies on clays in natural estuaries (Shiozowa, 1970; Edzwald and O'Melia, 1975). However, the differential settling in estuarine environments does not rely solely on chemical changes of the water column, but alsos on the nature, size, density and buoyancy of clay particles (e.g., Mélières, 1973; Chamley, 1989). These phenomenons have been studied in the Guadalquivir River where Mélières (1973) evidenced the preferential settling of illite compared with smectite in the estuary. However, the influence of differential settling of clays on the Cadiz CDS appears to be neglegible. Indeed, selective flocculation processes occur mainly at the freshwater−/ea. water transition where rapid changes affect the salinity gradient (e.g., Chamley, 1989) and are not observed in the open ocean where hydrological properties between water masses are reduced as is the case for the MOW_L and MOW_U (Sánchez-Leal et al., 2017).

Some authors highlighted that the enrichment of some clay minerals in continental slope or abyssal plain sediments is likely the result of rapid aggregation and vertical transfer of clay particles due to their interaction with amorphous organic matter (Honjo, 1982; Honjo et al., 1982). Such a phenomenon can hardly exert a main control on clay mineral sedimentation patterns over the Gulf of Cadiz CDS since planktonic productivity in the area is not particular strong. Moreover, the contribution of this rapid vertical sinking to deep sea sedimentation is often less important quantitatively compared with advection through surface and bottom currents (Chamley, 1989).

The addition of smectite derived from volcanic rock and hydrothermal alteration is considered unlikely, given the distance between the slope of the Gulf of Cadiz and the closest source of hydrothermally-derived clay minerals, i.e., the North Atlantic ridge. Similarly, any contribution of nearby Gulf of Cadiz mud volcanoes is unlikely, since they are mostly enriched in illite and kaolinite (Martín-Puertas et al., 2007). In addition, even when hydrothermal sources are close, high terrigenous influxes from the coast have more influence on clay association than fine particles from hydrothermal origin (e.g., Chamley, 1989).

The formation of authigenic smectite due to the oxidation of biogenic silica by Fe-oxydroxides in the cold water column (Cole and Shaw, 1983; and references therein) is not considered a major source of smectite in the Gulf of Cadiz.

Several studies on the size distribution of the clay minerals carried to the ocean describe smectite as the smallest (~0.4 µm) clay mineral while kaolinite is larger (~2 µm; Gibbs, 1967; Johnson and Kelley, 1984). In addition, the shape, buoyancy and electrochemical characteristics of these clay minerals entail that even small-sized kaolinite settles more

rapidly than smectite (Chamley, 1989). Indeed, smectite particles are characterized by a low density and high buoyancy resulting in particularly slow settling rates (10 times slower than kaolinite or illite) in the open ocean (Chamley, 1989). We propose that the difference of clay mineral composition observed between the drifts of the Gulf of Cadiz probably results from the differential deposition of clay minerals according to their size during their transport by currents, as initially proposed by Gibbs (1977) for sediments delivered by the Amazon River. The relatively rapid sinking of kaolinite minerals in the water column may lead to higher kaolinite concentrations in the lower branch of the MOW, ultimately leading to higher kaolinite content in drifts located in the path of MOW_L (Fig. 10). Inversely, small smectite particles sink more slowly and are therefore more abundant in the shallower sections of the MOW.This seggregation may explain the high abundance of smectite on the Huelva Drift (644 mbsl), located under the shallowest section of the MOW_{prox} (Sánchez-Leal et al., 2017), and on the Faro Drift (560 mbsl), under the MOW_U (Fig. 9). Consequently, smectites are exported by the MOW considerably further than kaolinite, notably along Portuguese margins where the alongslope sedimentation is seemingly controlled by clay minerals transported by the MOW (Grousset et al., 1988; Schönfeld, 1997; Stumpf et al., 2011; Fig. 10).

5.4. *Evolution of clay mineral deposition over the last glacial-interglacial cycle in the CDS of the Gulf of Cadiz*

In line with previous work on clay minerals in the Gulf of Cadiz (Grousset et al., 1988; López-Galindo et al., 1999; Stumpf et al., 2011), we find that clay mineral composition in the middle slope is a mixture between African and south Iberian sources, allowing us to identify a Northwest African an eastern Cadiz pole as specific endmembers (Fig. 6). Our records from IODP sites U1386, U1389 and U1390 display significant variations in clay mineral assemblages over the last 25 kyrs, which are likely related to the influence of respective sources and transport patterns. Considering the short time interval studied (25 kyrs), we do not consider the long-term, climate controlled formation of clays in soils as a significant contributing factor to changes in clay mineral assemblages at our study sites (Thiry, 2000).

Between 25 and 18 kyrs cal. BP, clay mineral assemblages in our records are almost constant (Figs. 3–5) and theyplot between the two

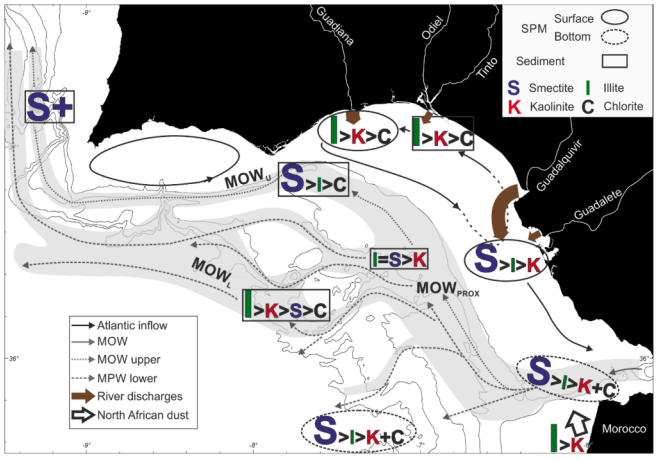

Fig. 10. Schematic source-to-sink pathways of clay minerals in the Gulf of Cadiz from river discharge and eolian inputs to their deposition on drifts in the Gulf of Cadiz. The size of the brown arrows is proportional to the contribution of the rivers to clay sedimentation in the Gulf of Cadiz. The schematic map contains only clay mineral abundances >10%. The size of the letters representing the clay minerals is proportional to their abundance. MOW: Mediterranean Outflow Water; SPM: Suspended Particulate Matter. (For interpretation of the references to colour in this figure legend, the reader is referred to the web version of this article.)

end-members previously identified (Figs. 6 and 11). Consequently, we suggest that the influence of both Northwest African and south Iberian sources were relatively stable during this cold period. Together with the homogenous clay mineral assemblages, strong similarities between the Alboran ODP Site 976, IODP Site U1390 and CADISAR cores located along the path of MOW_L (Fig. 11), as well as discrepancies between IODP sites located under the proximal and the upper MOW, reflect the dominant control of MOW on clay mineral sedimentation. This cold period is characterized by high and stable smectite-to-kaolinite ratio (S/K) for each IODP site (Fig. 12). The highest of S/K ratios are observed at IODP Site U1386 (S/K = 11). IODP Site U1389 displays lower S/K ratios (S/K = 6), while IODP Site U1390 is characterized by the lowest S/K ratio (S/K = 2) throughout this cold period. This strongly supports our hypothesis of physical sorting of clay minerals by size between the distinct MOW branches. Indeed, the S/K range of values contrast with those of the Guadiana River (S/K = 0), Guadalquivir River (S/K = 4) and even of the Northwest African pole (S/K = 1), which are considered as the main fine-grained particle suppliers in the Gulf of Cadiz.

S/K and I/K ratios show an average decrease from MIS2 to present day except at IODP Site U1389 (Fig. 12), due to a decrease of smectite content in IODP Site U1386 and an increase of kaolinite abundance at IODP Site U1390 as revealed by XRD patterns. Stumpf et al. (2011) found a similar behaviour for smectite, illite and kaolinite content over the last 22 kyrs near the study area. Together with these results, our records of enriched smectite during MIS2 suggest a stronger (lower) influence of Guadalquivir River (the North African pole) discharge during the MIS2 than during the Holocene. Several studies demonstrate that south Iberian temperatures and precipitations were unexpectedly close to present-day conditions during Dansgaard-Oeschger interstadials, including the 21–17.5 kyrs cal. BP period (Sánchez-Goñi et al., 2002; Turon et al., 2003; Nebout et al., 2009), ruling out any modification of river discharge due to modified hydrological conditions on their main drainage area. During the MIS2, the mouths of south Iberian rivers were located further offshore closerr to the Cadiz CDS due to the lowe relative sea-level (−105/−123 m below present day sea level; Waelbroeck et al., 2002). This may have modified the influence of the Guadalquivir River by reducing the distance travelled by clay minerals before their deposition. Furthermore, previous studies have evidenced a mean shallower depth of the MOW during the present interglacial than during the last glacial cold period (Schönfeld and Zahn, 2000; Rogerson et al., 2005, 2012; Llave et al., 2006). This observation, together with our clay mineral segregation findings (smectite-rich MOW_U vs. kaolinite-rich MOW_L), may explain the enhanced contribution of kaolinite (smectite) during MIS1 (MIS2) to the CDS via the general shallower distribution of both branches of the MOW (MOW_U and MOW_L) during interglacials than during glacial periods.

The overall decrease of illite-to kaolinite ratio (I/K) over the last 25 kyrs in the Gulf of Cadiz (Fig. 12), can be interpreted in the context of the latitudinal migration of Saharan dust sources with the intertropical convergence zone (ITCZ) and insolation-driven continental climatic variations (Caquineau et al., 1998; Skonieczny et al., 2011, 2013; Stumpf et al., 2011). Previous studies in the Mediterranean Sea evidenced an abrupt transition from Saharan-sourced dust during MIS2 to Sahelian-sourced dust during MIS1 (Bout-Roumazeilles et al., 2007, 2013). The higher I/K ratios characterizing MIS2 in the Gulf of Cadiz (Fig. 12) thus likely reflect the dominant influence of Saharan v. Sahelian sources in the Western Mediterranean during cold climatic periods, while the overall decrease in I/K ratios reflects the progressive southward migration of the ITCZ during the late Holocene (Stumpf et al., 2011; Bout-Roumazeilles et al., 2013). I/K ratios remain relatively stable toward the end of the African Humid Period (Fig. 12), which is characterized by the deposition of Sapropel 1 in the Western Mediterranean (10–6 kyrs cal. BP), and is generally associated with a weak MOW (Voelker et al., 2006; Toucanne et al., 2007; Rogerson et al., 2012; Kaboth et al., 2016). During this period of reduced MOW, we observe that the mineralogical composition from the Faro Drift, along with those

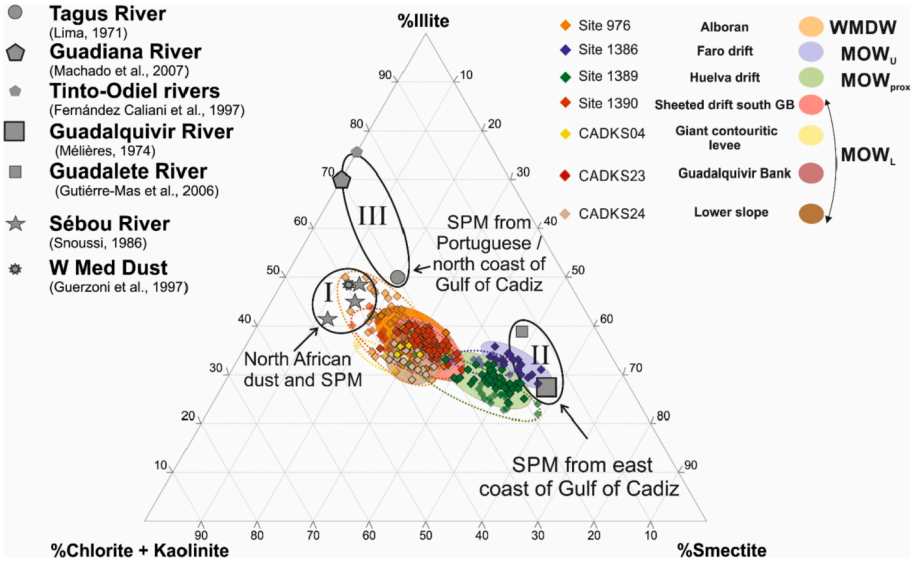

Fig. 11. Smectite vs. illite vs. chlorite + kaolinite ternary plot for samples covering the Last Glacial Maximum (18–25 kyrs cal. BP) from the Gulf of Cadiz and Alboran Sea (Bout-Roumazeilles et al., 2007). Endemembers are derived from previous published records and are divided intp three groups: North African dust and SPM (I), SPM from the eastern pole of the Gulf of Cadiz (II) and SPM from the northern pole of the Gulf of Cadiz (III). Lighter coloured rombs and dotted ellipses represent samples for the last 5 kyrs. SPM: Suspended Particle Matter; WMDW: Western Mediterranean Deep Water; MOW: Mediterranean Outflow Water; MOW$_U$: upper branch of the MOW; MOW$_{PROX}$: proximal MOW; MOW$_L$: lower branch of the MOW.

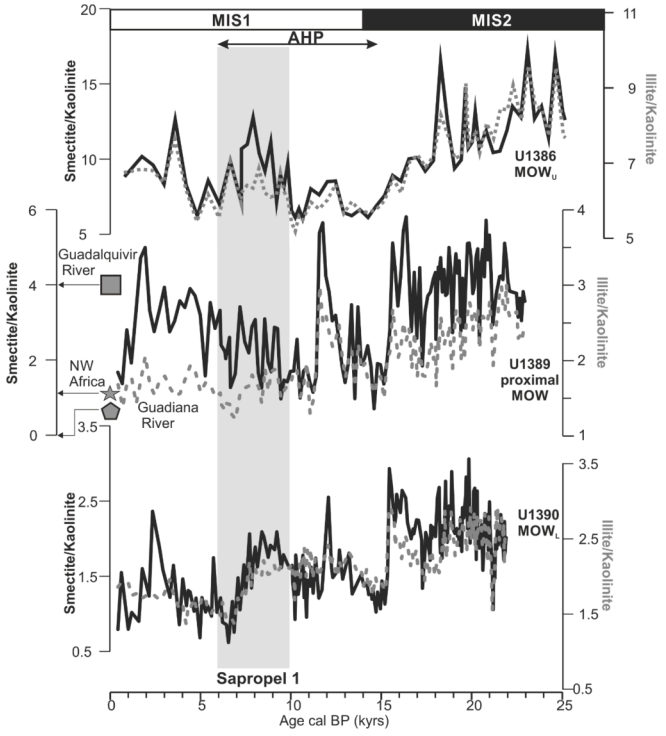

Fig. 12. Smectite/Kaolinite (S/K) and Illite/Kaolinite (I/K) ratios on IODP sites influenced by the upper core of Mediterranean Outflow Water (MOW$_U$), lower core of the Mediterranean Outflow Water (MOW$_L$) and both (MOW$_{PROX}$), over the last 25 kyrs. The grey square and pentagon represent the S/K values of clay assemblages from Suspended Particulate Matter in the Guadanlquivir River and Guadiana River, respectively (Mélières, 1973; Machado et al., 2007). The S/K value of the Northern African pole is marked by a grey star (Snoussi, 1986; Guerzoni et al., 1997; Elmouden et al., 2005). MIS: Marine Isotope Stage; AHP: African Humid Period.

from other drifts, remains distinctly different from that of the Guadiana river (Fig. 12), the nearest with a significant sediment discharge. Consequently, we suggest that both branches of the MOW, despite their lower activity, continue to redistribute fine-grained particles and influence clay mineral distribution in the middle slope of the Gulf of Cadiz.

6. Conclusions

This multisite study with high resolution records focuses for the first time on clay mineral distribution along the Contourite Depositional System (CDS) of the Gulf of Cadiz. The extensive review of literature on clay minerals presented in this study enables us to identify the different sources of clay particles across the middle slope. Our records show that fine-grained sediments of the CDS reflect mainly a mixture between clay particles from rivers located east of the Gulf of Cadiz, especially the Guadalquivir River, and clay mineral assemblages from dusts, soils and rivers from Northwestern Africa. However, the combined influence of cyclonic eddies on the northern continental shelf and Mediterranean Outflow Water (MOW), which flows along the middle slope, prevents the export of clay mineral particles from the Guadiana and Tinto-Odiel Rivers to the CDS of the Gulf of Cadiz.

In addition to forming an effective barrier against offshore clay export, the present day MOW carries similar Suspended Particulate Matter (SPM) concentrations in its upper and lower branches and plays a pivotal role in fine particles supply to the middle slope of the Gulf of Cadiz. The contrasted sedimentation rates observed on the Faro, Huelva and sheeted Drifts southeast of the Guadalquivir Bank are probably indicative of varying SPM concentrations for the upper and lower MOW over the last 25 kyrs.

The MOW plays a critical role in redistributing fine-grained particles sourced by rivers to the east of the Gulf of Cadiz and the Alboran Sea through the settling of clay minerals along the CDS. This study shows that the lateral variations in clay mineralogy in the middle slope are the result of size segregation deposition processes during the transport of clay minerals by the MOW. Consequently, clay associations in marine sediments are pertinent proxies for the mapping of the pathways of the upper and lower MOW in the Gulf of Cadiz, while also tracing the Mediterranean water masses along the Portuguese margins.

The contribution of both northwest African dusts and south Iberian rivers to the composition of fine-grained particles in the middle slope of the Gulf of Cadiz has varied over the last 25 kyrs. The relatively low sea-level which characterized the Last Glacial Maximum brought the South Iberian river mouths closer to the CDS, enhancing the influence of Guadalquivir River particle-derived sedimentation across the middle slope during this cold period. Vertical variation of the MOW from MIS2 to MIS1, induced a shallowing of the upper and lower cores of the MOW, which may explain the difference in clay mineral association between these time intervals. Furthermore, the progressive southward migration of the intertropical convergence zone during the Holocene induced the

latitudinal migration of Saharan dust sources and influenced sedimentation in the Gulf of Cadiz.

The present study offers a high-resolution rcord of source-to-sink pathways of clay minerals, from the Northwest African and South Iberian sources to their settling in the Gulf of Cadiz CDS via surface and bottom currents. This re-construction of clay mineral pathways aims to provide a strong basis for future investigations on fine particles settling over the CDS at larger time scales.Indeed, the study of clay minerals may lead to a better understanding of sedimentary drift evolution by identifying the influence of various sources, modes of transport and sedimentation processes of fine particles. Moreover, the contrasted clay mineral associations observed between the paths of the MOW_U and the MOW_L may serve as a tracer of vertical shifts in both branches of the MOW as far back as onset of contourite deposition in the Gulf of Cadiz during the lower Pliocene.

Data availability

Moal-Darrigade, Paul; Ducassou, Emmanuelle; Bout-Roumazeilles, Viviane; Hanquiez, Vincent; Perello, Marie-Claire; Mulder, Thierry; Giraudeau, Jacques (2021), "Clay minerals in the Cadiz contourite system over the last 25 kyrs ", Mendeley Data, V3, doi: 10.17632/8h9cfjkdpg.3

https://data.mendeley.com/datasets/8h9cfjkdpg/draft?a=6b57f86a-8a28-45de-9d3e-b217f6ac6a5a

Declaration of Competing Interest

The authors declare that they have no known competing financial interests or personal relationships that could have appeared to influence the work reported in this paper.

Acknowledgements

P. Moal-Darrigade is supported by a doctoral scholarship from French Ministry of Research. The authors warmly thank IODP Expedition 339 and CADISAR crew and scientific teams of onboard the *Joides Resolution* and the r/v le Suroît, for the recovery of the studied material. We are grateful to the French INSU LEFE programme (MOWCA project) for financial support. We thank Eleanor Georgiadis for very significant help in the language improvement of this paper. We would like finally to thank Pr Dorrik Stow (Guest Editor), Dr. Sara Rodrigues and an anonymous reviewer, for their constructive comments that helped us improve the manuscript.

References

Achab, M., 2011. Dynamics of sediments exchange and transport in the bay of cadiz and the adjacent continental shelf (SW - Spain). In: Manning, A. (Ed.), Sediment Transport in Aquatic Environments. InTech. https://doi.org/10.5772/20652.

Achab, M., Gutierrez-Mas, J.M., Aguayo, F.L., 2008. Utility of clay minerals in the determination of sedimentary transport patterns in the Bay of Cadiz. Geodin. Acta 21, 259–272. https://doi.org/10.3166/ga.21.259-272.

Alonso, B., Maldonado, A., 1990. Late Quaternary sedimentation patterns of the Ebro turbidite systems (northwestern Mediterranean): two styles of deep-sea deposition. Mar. Geol. 95, 353–377. https://doi.org/10.1016/0025-3227(90)90124-3.

Alonso, B., Ercilla, G., Casas, D., Stow, D.A.V., Rodríguez-Tovar, F.J., Dorador, J., Hernández-Molina, F.-J., 2016. Contourite vs gravity-flow deposits of the Pleistocene Faro Drift (Gulf of Cadiz): Sedimentological and mineralogical approaches. Mar. Geol. 377, 77–94. https://doi.org/10.1016/j.margeo.2015.12.016.

Ambar, I., Howe, M.R., 1979. Observations of the Mediterranean outflow–II The deep circulation in the vicinity of the Gulf of Cadiz. Deep Sea Res. Part Oceanogr. Res. Pap. 26, 535–554. https://doi.org/10.1016/0198-0149(79)90095-5.

Ambar, I., Serra, N., Brogueira, M.J., Cabeçadas, G., Abrantes, F., Freitas, P., Gonçalves, C., Gonzalez, N., 2002. Physical, chemical and sedimentological aspects of the Mediterranean outflow off Iberia. Deep Sea Res. Part II Top. Stud. Oceanogr. 49, 4163–4177. https://doi.org/10.1016/S0967-0645(02)00148-0.

Auffret, G.-A., Pastouret, L., Chamley, H., Lanoix, F., 1974. Influence of the prevailing current regime on sedimentation in the Alboran Sea. Deep-Sea Res. Oceanogr. Abstr. 21, 839–849. https://doi.org/10.1016/0011-7471(74)90003-5.

Avila, A., Queralt-Mitjans, I., Alarcón, M., 1997. Mineralogical composition of African dust delivered by red rains over northeastern Spain. J. Geophys. Res.-Atmos. 102, 21977–21996. https://doi.org/10.1029/97JD00485.

Avila, A., Alarcón, M., Queralt, I., 1998. The chemical composition of dust transported in red rains—its contribution to the biogeochemical cycle of a holm oak forest in Catalonia (Spain). Atmos. Environ. 32, 179–191. https://doi.org/10.1016/S1352-2310(97)00286-0.

Bahr, A., Jiménez-Espejo, F.J., Kolasinac, N., Grunert, P., Hernández-Molina, F.J., Röhl, U., Voelker, A.H.L., Escutia, C., Stow, D.A.V., Hodell, D., Alvarez-Zarikian, C. A., 2014. Deciphering bottom current velocity and paleoclimate signals from contourite deposits in the Gulf of Cádiz during the last 140 kyr: an inorganic geochemical approach. Geochem. Geophys. Geosyst. 15, 3145–3160. https://doi.org/10.1002/2014GC005356.

Bahr, A., Kaboth, S., Jiménez-Espejo, F.J., Sierro, F.J., Voelker, A.H.L., Lourens, L., Röhl, U., Reichart, G.J., Escutia, C., Hernández-Molina, F.J., Pross, J., Friedrich, O., 2015. Persistent monsoonal forcing of Mediterranean Outflow Water dynamics during the late Pleistocene. Geology 43, 951–954. https://doi.org/10.1130/G37013.1.

Baldy, P., Boillot, G., Dupeuble, P., Malod, J., Moita, I., Mougenot, D., 1977. Carte géologique du plateau continental sud-portugais et sud-espagnol (Golfe de Cadix). Bull. Soc. Geol. Fr. 7, 703–724. https://doi.org/10.2113/gssgfbull.S7-XIX.4.703.

Bankole, S., Buckman, J., Stow, D., 2020. Unusual components within a fine-grained contourite deposit: significance for interpretation of provenance and the contourite budget. Minerals 10, 488. https://doi.org/10.3390/min10060488.

Baringer, M.O., Price, J.F., 1999. A review of the physical oceanography of the Mediterranean outflow. Mar. Geol. 155, 63–82. https://doi.org/10.1016/S0025-3227(98)00141-8.

Bellanco, M.J., Sánchez-Leal, R.F., 2016. Spatial distribution and intra-annual variability of water masses on the Eastern Gulf of Cadiz seabed. Cont. Shelf Res. 128, 26–35. https://doi.org/10.1016/j.csr.2016.09.001.

Biscaye, P.E., Eittreim, S.L., 1977. Suspended particulate loads and transports in the nepheloid layers of the abyssal Atlantic Ocean. Mar. Geol. 23, 155–172.

Bout-Roumazeilles, V., Cortijo, E., Labeyrie, L., Debrabant, P., 1999. Clay mineral evidence of nepheloid layer contributions to the Heinrich layers in the Northwest Atlantic. Palaeogeogr. Palaeoclimatol. Palaeoecol. 146, 211–228. https://doi.org/10.1016/S0031-0182(98)00137-0.

Bout-Roumazeilles, V., Combourieu Nebout, N., Peyron, O., Cortijo, E., Landais, A., Masson-Delmotte, V., 2007. Connection between South Mediterranean climate and North African atmospheric circulation during the last 50,000yrBP North Atlantic cold events. Quat. Sci. Rev. 26, 3197–3215. https://doi.org/10.1016/j.quascirev.2007.07.015.

Bout-Roumazeilles, V., Riboulleau, A., du Châtelet, E.A., Lorenzoni, L., Tribovillard, N., Murray, R.W., Müller-Karger, F., Astor, Y.M., 2013. Clay mineralogy of surface sediments as a tool for deciphering river contributions to the Cariaco Basin (Venezuela). J. Geophys. Res. Oceans 118, 750–761. https://doi.org/10.1002/jgrc.20079.

Brackenridge, R.E., Stow, D.A.V., Hernández-Molina, F.J., Jones, C., Mena, A., Alejo, I., Ducassou, E., Llave, E., Ercilla, G., Nombela, M.A., Perez-Arlucea, M., Frances, G., 2018. Textural characteristics and facies of sand-rich contourite depositional systems. Sedimentology 65, 2223–2252. https://doi.org/10.1111/sed.12463.

Brown, G., 1980. X-ray diffraction procedures for clay mineral identification. Cryst. Struct. Clay Miner. Their X-Ray Identif. 305–359.

Bryden, H.L., Stommel, H.M., 1984. Limiting processes. Oceanol. Acta 7, 289–296.

Bryden, H.L., Candela, J., Kinder, T.H., 1994. Exchange through the strait of gibraltar. Prog. Oceanogr. 33, 201–248. https://doi.org/10.1016/0079-6611(94)90028-0.

Cacho, I., Grimalt, J.O., Sierro, F.J., Shackleton, N., Canals, M., 2000. Evidence for enhanced Mediterranean thermohaline circulation during rapid climatic coolings. Earth Planet. Sci. Lett. 183, 417–429. https://doi.org/10.1016/S0012-821X(00)00296-X.

Caquineau, S., Gaudichet, A., Gomes, L., Magonthier, M.-C., Chatenet, B., 1998. Saharan dust: Clay ratio as a relevant tracer to assess the origin of soil-derived aerosols. Geophys. Res. Lett. 25, 983–986. https://doi.org/10.1029/98GL00569.

Caquineau, S., Gaudichet, A., Gomes, L., Legrand, M., 2002. Mineralogy of Saharan dust transported over northwestern tropical Atlantic Ocean in relation to source regions. J. Geophys. Res.-Atmos. 107 https://doi.org/10.1029/2000JD000247. AAC 4-1-AAC 4-12.

Carracedo, L.I., Pardo, P.C., Flecha, S., Pérez, F.F., 2016. On the mediterranean water composition. J. Phys. Oceanogr. 46, 1339–1358. https://doi.org/10.1175/JPO-D-15-0095.1.

Chamley, H., 1989. Clay Sedimentology. Springer.

Cole, T., Shaw, H., 1983. The nature and origin of authigenic smectites in some recent marine sediments. Clay Miner. 18, 239–252. https://doi.org/10.1180/claymin.1983.018.3.02.

Colmenero-Hidalgo, E., Flores, J.-A., Sierro, F.J., Bárcena, M.Á., Löwemark, L., Schönfeld, J., Grimalt, J.O., 2004. Ocean surface water response to short-term climate changes revealed by coccolithophores from the Gulf of Cadiz (NE Atlantic) and Alboran Sea (W Mediterranean). Palaeogeogr. Palaeoclimatol. Palaeoecol. 205, 317–336. https://doi.org/10.1016/j.palaeo.2003.12.014.

De Castro, S., Hernandez-Molina, F.J., Rodriguez-Tovar, F.J., Llave, E., Ng, Z.L., Nishida, N., Mena, A., 2020. Contourites and bottom current reworked sands_ Bed facies model and implications. Mar. Geol. 428, 106267 https://doi.org/10.1016/j.margeo.2020.106267.

De Castro, S., Hernandez-Molina, F.J., De Weger, W., Jimenez-Espejo, F.J., Rodriguez-Tovar, F.J., Mena, A., Llave, E., Sierro, F.J., 2021. Contourite characterization and its discrimination from other deep-water deposits in the Gulf of Cadiz contourite depositional system. Sedimentology 68, 987–1027.

Ducassou, E., Hassan, R., Gonthier, E., Duprat, J., Hanquiez, V., Mulder, T., 2018. Biostratigraphy of the last 50 kyr in the contourite depositional system of the Gulf of Cádiz. Mar. Geol. 395, 285–300. https://doi.org/10.1016/j.margeo.2017.09.014.

Edzwald, J.K., O'Melia, C.R., 1975. Clay distributions in recent estuarine sediments. Clay Clay Miner. 23, 39–44. https://doi.org/10.1346/CCMN.1975.0230106.

Elbaz-Poulichet, F., Morley, N.H., Beckers, J.-M., Nomerange, P., 2001. Metal fluxes through the Strait of Gibraltar: the influence of the Tinto and Odiel rivers (SW Spain). Mar. Chem. 73, 193–213. https://doi.org/10.1016/S0304-4203(00)00106-7.

Elmouden, A., Bouchaou, L., Snoussi, M., 2005. Constraints on alluvial clay mineral assemblages in semiarid regions. The Souss Wadi Basin (Morocco, Northwestern Africa). Geol. Acta 3, 3–14. https://doi.org/10.1344/105.000001410.

Ercilla, G., Juan, C., Hernández-Molina, F.J., Bruno, M., Estrada, F., Alonso, B., Casas, D., Farran, Marcel, Lí Llave, E., García, M., Vázquez, J.T., D'Acremont, E., Gorini, C., Palomino, D., Valencia, J., El Moumni, B., Ammar, A., 2016. Significance of bottom currents in deep-sea morphodynamics: an example from the Alboran Sea. Mar. Geol. 378, 157–170. https://doi.org/10.1016/j.margeo.2015.09.007.

Faugères, J.-C., Gonthier, E., Stow, D.A.V., 1984. Contourite drift molded by deep mediterranean outflow. Geology 12, 296–300. https://doi.org/10.1130/0091-7613(1984)12<296:CDMBDM>2.0.CO;2.

Faugères, J.-C., Gonthier, E., Peypouquet, J., Pujol, C., Vergnaud-Grazzini, C., 1986. Distribution et variations des courants de fond sur la ride de Faro (Golfe de Cadix), témoins des modifications des échanges Méditerranée-Atlantique au Quaternaire récent. Bull. Société Géologique Fr. 2, 423–432. https://doi.org/10.2113/gssgfbull.II.3.423.

Fernández-Caliani, J.C., Ruiz-Muñoz, F., Galán, E., 1997. Clay mineral and heavy metal distributions in the lower estuary of Huelva and adjacent Atlantic shelf, SW Spain. Sci. Total Environ. 198, 181–200. https://doi.org/10.1016/S0048-9697(97)05450-8.

Fernández-Nóvoa, D., deCastro, M., Des, M., Costoya, X., Mendes, R., Gómez-Gesteira, M., 2017. Characterization of Iberian turbid plumes by means of synoptic patterns obtained through MODIS imagery. J. Sea Res. 126, 12–25. https://doi.org/10.1016/j.seares.2017.06.013.

Formenti, P., Rajot, J.L., Desboeufs, K., Caquineau, S., Chevaillier, S., Nava, S., Gaudichet, A., Journet, E., Triquet, S., Alfaro, S., Chiari, M., Haywood, J., Coe, H., Highwood, E., 2008. Regional variability of the composition of mineral dust from western Africa: results from the AMMA SOP0/DABEX and DODO field campaigns. J. Geophys. Res.-Atmos. 113 https://doi.org/10.1029/2008JD009903.

Freitas, M.C., Andrade, C., Moreno, J.C., Munhá, J.M., Cachão, M., 1998. The sedimentary record of recent (last 500 years) environmental changes in the Seixal Bay marsh, Tagus estuary, Portugal. Geol. En Mijnb. 77, 283–293. https://doi.org/10.1023/A:1003695022853.

Freitas, P.S., Abrantes, F., 2002. Suspended particulate matter in the Mediterranean water at the Gulf of Cadiz and off the southwest coast of the Iberian Peninsula. Deep Sea Res. Part II Top. Stud. Oceanogr. 49, 4245–4261. https://doi.org/10.1016/S0967-0645(02)00153-4.

García, M., 2002. Caracterización Morfológica del Sistema de Canales y de Valles Submarinosdel Talud Medio del Golfo de Cádiz (SO de la Península Ibérica): Implicaciones Oceanográficas. Tesis de Licenciatura. Facultad de Ciescias del Mar, Universidad de Cádiz.

García, M., Hernández-Molina, F.J., Llave, E., Stow, D.A.V., León, R., Fernández-Puga, M. C., Diaz del Río, V., Somoza, L., 2009. Contourite erosive features caused by the Mediterranean Outflow Water in the Gulf of Cadiz: Quaternary tectonic and oceanographic implications. Mar. Geol. 257, 24–40. https://doi.org/10.1016/j.margeo.2008.10.009.

García, M., Hernández-Molina, F.J., Alonso, B., Vázquez, J.T., Ercilla, G., Llave, E., Casas, D., 2016. Erosive sub-circular depressions on the Guadalquivir Bank (Gulf of Cadiz): interaction between bottom current, mass-wasting and tectonic processes. Mar. Geol. 378, 5–19. https://doi.org/10.1016/j.margeo.2015.10.004.

García, M., Llave, E., Hernández-Molina, F.J., Lobo, F.J., Ercilla, G., Alonso, B., Casas, D., Mena, A., Fernández-Salas, L.M., 2020. The role of late Quaternary tectonic activity and sea-level changes on sedimentary processes interaction in the Gulf of Cadiz upper and middle continental slope (SW Iberia). Mar. Pet. Geol. 121, 104595 https://doi.org/10.1016/j.marpetgeo.2020.104595.

García-Lafuente, J., Delgado, J., Criado-Aldeanueva, F., Bruno, M., del Río, J., Miguel Vargas, J., 2006. Water mass circulation on the continental shelf of the Gulf of Cádiz. Deep Sea Res. Part II Top. Stud. Oceanogr. 53, 1182–1197. https://doi.org/10.1016/j.dsr2.2006.04.011.

Gasser, M., Pelegrí, J.L., Emelianov, M., Bruno, M., Gràcia, E., Pastor, M., Peters, H., Rodríguez-Santana, Á., Salvador, J., Sánchez-Leal, R.F., 2017. Tracking the Mediterranean outflow in the Gulf of Cadiz. Prog. Oceanogr. 157, 47–71. https://doi.org/10.1016/j.pocean.2017.05.015.

Gibbs, R.J., 1967. The geochemistry of the Amazon River system: part I. The factors that control the salinity and the composition and concentration of the suspended solids. Geol. Soc. Am. Bull. 78, 1203–1232. https://doi.org/10.1130/0016-7606(1967)78[1203:TGOTAR]2.0.CO;2.

Gibbs, R.J., 1977. Clay mineral segregation in the marine environment. SEPM J. Sediment. Res. 47, 237–243. https://doi.org/10.1306/212F713A-2B24-11D7-8648000102C1865D.

Gonthier, E., Faugères, J.-C., Stow, D., 1984. Contourite facies of the Faro drift, Gulf of Cadiz. Geol. Soc. Lond. Spec. Publ. 15, 275–292. https://doi.org/10.1144/GSL.SP.1984.015.01.18.

Gonzalez, R., Dias, J.M.A., Lobo, F., Mendes, I., 2004. Sedimentological and paleoenvironmental characterisation of transgressive sediments on the Guadiana Shelf (Northern Gulf of Cadiz, SW Iberia). Quat. Int. 120, 133–144. https://doi.org/10.1016/j.quaint.2004.01.012.

Goudie, A.S., Middleton, N.J., 2001. Saharan dust storms: nature and consequences. Earth-Sci. Rev. 56, 179–204. https://doi.org/10.1016/S0012-8252(01)00067-8.

Grousset, F.E., Joron, J.L., Biscaye, P.E., Latouche, C., Treuil, M., Maillet, N., Faugères, J. C., Gonthier, E., 1988. Mediterranean outflow through the Strait of Gibraltar since 18,000 years B.P.: mineralogical and geochemical arguments. Geo-Mar. Lett. 8, 25–34. https://doi.org/10.1007/BF02238003.

Grousset, F.E., Rognon, P., Coudé-Gaussen, G., Pédemay, P., 1992. Origins of peri-Saharan dust deposits traced by their Nd and Sr isotopic composition. Palaeogeogr. Palaeoclimatol. Palaeoecol. 93, 203–212. https://doi.org/10.1016/0031-0182(92)90097-O.

Guerzoni, S., Molinaroli, E., Chester, R., 1997. Saharan dust imputs to the W. Mediterranean Sea: depositional patterns, geochemistry and sedimentological implications. Deep Sea Res. Part II Top. Stud. Oceanogr. 44, 631–654. https://doi.org/10.1016/S0967-0645(96)00096-3.

Gutiérrez-Mas, J.M., López-Galindo, A., López-Aguayo, F., 1997. Clay minerals in recent sediments of the continental shelf and the Bay of Cadiz (SW Spain). Clay Miner. 32, 507–515.

Gutiérrez-Mas, J.M., Moral, J.P., Sánchez, A., Dominguez, S., Muñoz-Perez, J.J., 2003. Multicycle sediments on the continental shelf of Cadiz (SW Spain). Estuar. Coast. Shelf Sci. 57, 667–677. https://doi.org/10.1016/S0272-7714(02)00407-9.

Gutiérrez-Mas, J.M., López-Aguayo, F., Achab, M., 2006. Clay minerals as dynamic tracers of suspended matter dispersal in the Gulf of Cadiz (SW Spain). Clay Miner. 41, 727–738. https://doi.org/10.1180/0009855064130215.

Habgood, E.L., Kenyon, N.H., Masson, D.G., Akhmetzhanov, A., Weaver, P.P.E., Gardner, J., Mulder, T., 2003. Deep-water sediment wave fields, bottom current sand channels and gravity flow channel-lobe systems: Gulf of Cadiz, NE Atlantic: sediment deposition in the Gulf of Cadiz. Sedimentology 50, 483–510. https://doi.org/10.1046/j.1365-3091.2003.00561.x.

Hanquiez, V., Mulder, T., Lecroart, P., Gonthier, E., Marchès, E., Voisset, M., 2007. High resolution seafloor images in the Gulf of Cadiz, Iberian margin. Mar. Geol. 246, 42–59. https://doi.org/10.1016/j.margeo.2007.08.002.

Hanquiez, V., Mulder, T., Toucanne, S., Lecroart, P., Bonnel, C., Marchès, E., Gonthier, E., 2010. The sandy channel–lobe depositional systems in the Gulf of Cadiz: gravity processes forced by contour current processes. Sediment. Geol. 229, 110–123. https://doi.org/10.1016/j.sedgeo.2009.05.008.

Hassan, R., 2014. La Sédimentation Dans le Golfe de Cadix au cours des Derniers 50 000 ans (Analyses Multi-Paramètres et Multi-échelles) (PhD Thesis). Universite de Bordeaux.

Hernández-Molina, F.J., Llave, E., Stow, D.A.V., García, M., Somoza, L., Vázquez, J.T., Lobo, F.J., Maestro, A., Díaz del Río, V., León, R., Medialdea, T., Gardner, J., 2006. The contourite depositional system of the Gulf of Cádiz: a sedimentary model related to the bottom current activity of the Mediterranean outflow water and its interaction with the continental margin. Deep Sea Res. Part II Top. Stud. Oceanogr. 53, 1420–1463. https://doi.org/10.1016/j.dsr2.2006.04.016.

Hernández-Molina, F.J., Stow, D., Alvarez-Zarikian, C., Expedition IODP 339 Scientists, 2013. IODP Expedition 339 in the Gulf of Cadiz and off West Iberia: decoding the environmental significance of the Mediterranean outflow water and its global influence. Sci. Drill. 16, 1–11. https://doi.org/10.5194/sd-16-1-2013.

Hernández-Molina, F.J., Wåhlin, A., Bruno, M., Ercilla, G., Llave, E., Serra, N., Rosón, G., Puig, P., Rebesco, M., Van Rooij, D., Roque, D., González-Pola, C., Sánchez, F., Gómez, M., Preu, B., Schwenk, T., Hanebuth, T.J.J., Sánchez Leal, R.F., García-Lafuente, J., Brackenridge, R.E., Juan, C., Stow, D.A.V., Sánchez-González, J.M., 2016. Oceanographic processes and morphosedimentary products along the Iberian margins: a new multidisciplinary approach. Mar. Geol. 378, 127–156. https://doi.org/10.1016/j.margeo.2015.12.008.

Hernández-Molina, J., Llave, E., Somoza, L., Fernández-Puga, M.C., Maestro, A., León, R., Medialdea, T., Barnolas, A., García, M., del Río, V.D., Rodero, J., Gardner, J., 2003. Looking for clues to paleoceanographic imprints: a diagnosis of the Gulf of Cadiz contourite depositional systems. Geology 31, 19–22. https://doi.org/10.1130/0091-7613(2003)031<0019:LFCTPI>2.0.CO;2.

Honjo, S., 1982. Seasonality and interaction of biogenic and lithogenic particulate flux at the Panama Basin. Science 218, 883–884. https://doi.org/10.1126/science.218.4575.883.

Honjo, S., Manganini, S.J., Cole, J.J., 1982. Sedimentation of biogenic matter in the deep ocean. Deep Sea Res. Part Oceanogr. Res. Pap. 29, 609–625. https://doi.org/10.1016/0198-0149(82)90079-6.

Johnson, A.G., Kelley, J.T., 1984. Temporal, spatial, and textural variation in the mineralogy of Mississippi River suspended sediment. J. Sediment. Res. 54, 67–72. https://doi.org/10.1306/212F83A5-2B24-11D7-8648000102C1865D.

Jouanneau, J.M., Garcia, C., Oliveira, A., Rodrigues, A., Dias, J.A., Weber, O., 1998. Dispersal and deposition of suspended sediment on the shelf off the Tagus and Sado estuaries, S.W. Portugal. Prog. Oceanogr. 42, 233–257. https://doi.org/10.1016/S0079-6611(98)00036-6.

Kaboth, S., Bahr, A., Reichart, G.-J., Jacobs, B., Lourens, L.J., 2016. New insights into upper MOW variability over the last 150kyr from IODP 339 Site U1386 in the Gulf of Cadiz. Mar. Geol. 377, 136–145. https://doi.org/10.1016/j.margeo.2015.08.014.

Kaboth, S., Grunert, P., Lourens, L., 2017. Mediterranean Outflow Water variability during the early Pleistocene. Clim. Past 13, 1023–1035. https://doi.org/10.5194/cp-13-1023-2017.

Kandler, K., Schütz, L., Deutscher, C., Ebert, M., Hofmann, H., Jäckel, S., Jaenicke, R., Knippertz, P., Lieke, K., Massling, A., 2009. Size distribution, mass concentration, chemical and mineralogical composition and derived optical parameters of the boundary layer aerosol at Tinfou, Morocco, during SAMUM 2006. Tellus Ser. B Chem. Phys. Meteorol. 61, 32–50. https://doi.org/10.1111/j.1600-0889.2008.00385.x.

Kenyon, N.H., Belderson, R.H., 1973. Bed forms of the Mediterranean undercurrent observed with side-scan sonar. Sediment. Geol. 9, 77–99. https://doi.org/10.1016/0037-0738(73)90027-4.
Lima, L., 1971. Distribuição dos minerais argilosos na plataforma continental entre os cabos Raso e Espichel. In: Presented at the 1° Congresso Hispano-Luso-Americano de Geologia Económica, Madrid.
Llave, E., Hernandez-Molina, F.J., Somoza, L., Dıaz-del-Rıo, V., Stow, D.A.V., Maestro, A., Dias, J.M.A., 2001. Seismic stacking pattern of the Faro-Albufeira contourite system (Gulf of Cadiz): a Quaternary record of paleoceanographic and tectonic influences. Mar. Geophys. Reasearches 22, 487–508. https://doi.org/10.1023/A:1016355801344.
Llave, E., Schönfeld, J., Hernández-Molina, F.J., Mulder, T., Somoza, L., Díaz del Río, V., Sánchez-Almazo, I., 2006. High-resolution stratigraphy of the Mediterranean outflow contourite system in the Gulf of Cadiz during the late Pleistocene: the impact of Heinrich events. Mar. Geol. 227, 241–262. https://doi.org/10.1016/j.margeo.2005.11.015.
Llave, E., Hernández-Molina, F.J., Somoza, L., Stow, D., Del Río, V.D., 2007. Quaternary evolution of the contourite depositional system in the Gulf of Cadiz. Geol. Soc. Lond. Spec. Publ. 276, 49–79. https://doi.org/10.1144/GSL.SP.2007.276.01.03.
Lobo, F.J., Hernández-Molina, F.J., Somoza, L., Díaz del Río, V., 2001. The sedimentary record of the post-glacial transgression on the Gulf of Cadiz continental shelf (Southwest Spain). Mar. Geol. 178, 171–195. https://doi.org/10.1016/S0025-3227(01)00176-1.
Lofi, J., Voelker, A.H.L., Ducassou, E., Hernández-Molina, F.J., Sierro, F.J., Bahr, A., Galvani, A., Lourens, L.J., Pardo-Igúzquiza, E., Pezard, P., Rodríguez-Tovar, F.J., Williams, T., 2016. Quaternary chronostratigraphic framework and sedimentary processes for the Gulf of Cadiz and Portuguese Contourite depositional systems derived from natural gamma ray records. Mar. Geol. 377, 40–57. https://doi.org/10.1016/j.margeo.2015.12.005.
López-Galindo, A., Rodero, J., Maldonado, A., 1999. Surface facies and sediment dispersal patterns: southeastern Gulf of Cadiz, Spanish continental margin. Mar. Geol. 155, 83–98. https://doi.org/10.1016/S0025-3227(98)00142-X.
Machado, A., 2005. Geochemical characterization of surficial sediments from the southwestern Iberian continental shelf. Cienc. Mar. 31, 161–177. https://doi.org/10.7773/cm.v31i12.98.
Machado, A., Rocha, F., Gomes, C., Dias, J., 2007. Distribution and Composition of Suspended Particulate Matter in Guadiana Estuary (Southwestern Iberian Peninsula). J. Coast. Res. 6.
Madelain, F., 1970. Influence de la topographie du fond sur l'écoulement méditerranéen entre le Détroit de Gibraltar et le Cap Saint-Vincent. Cah. Océan. 22, 43–61.
Maldonado, A., Somoza, L., Pallarés, L., 1999. The Betic orogen and the Iberian–African boundary in the Gulf of Cadiz: geological evolution (central North Atlantic). Mar. Geol. 155, 9–43. https://doi.org/10.1016/S0025-3227(98)00139-X.
Marchès, E., Mulder, T., Cremer, M., Bonnel, C., Hanquiez, V., Gonthier, E., Lecroart, P., 2007. Contourite drift construction influenced by capture of Mediterranean Outflow Water deep-sea current by the Portimão submarine canyon (Gulf of Cadiz, South Portugal). Mar. Geol. 242, 247–260. https://doi.org/10.1016/j.margeo.2007.03.013.
Martín-Puertas, C., Mata, M.P., Fernández-Puga, M.C., Vázquez, J.T., Somoza, L., 2007. A comparative mineralogical study of gas-related sediments of the Gulf of Cádiz. Geo-Mar. Lett. 27, 223–235. https://doi.org/10.1007/s00367-007-0075-1.
McCave, I., Tucholke, B.E., 1986. Deep current-controlled sedimentation in the western North Atlantic. In: The Western North Atlantic Region. Geological Society of America, Boulder, Colorado, USA, pp. 451–468.
McCave, I.N., 1986. Local and global aspects of the bottom nepheloid layers in the world ocean. Neth. J. Sea Res. 20, 167–181. https://doi.org/10.1016/0077-7579(86)90040-2.
McCave, I.N., Manighetti, B., Robinson, S.G., 1995. Sortable silt and fine sediment size/composition slicing: parameters for palaeocurrent speed and palaeoceanography. Paleoceanography 10, 18. https://doi.org/10.1029/94PA03039.
Medialdea, T., Somoza, L., Pinheiro, L.M., Fernández-Puga, M.C., Vázquez, J.T., León, R., Ivanov, M.K., Magalhaes, V., Díaz-del-Río, V., Vegas, R., 2009. Tectonics and mud volcano development in the Gulf of Cádiz. Mar. Geol. 261, 48–63. https://doi.org/10.1016/j.margeo.2008.10.007.
Mélières, F., 1973. Les minéraux argileux de l'estuaire du Guadalquivir (Espagne). Bull. Groupe Fr. Argiles Tome 25 Fasc. 2, 1973. https://doi.org/10.3406/argil.1973.1192.
Mélières, F., 1974. Recherches sur la dynamique sedimentaire du Golfe de Cadix (Espagne) (PhD Thesis). Universite de Paris VI.
Milliman, J.D., Syvitski, J.P.M., 1992. Geomorphic/tectonic control of sediment discharge to the ocean: the importance of small mountainous rivers. J. Geol. 100, 525–544. https://doi.org/10.1086/629606.
Millot, C., 1999. Circulation in the Western Mediterranean Sea. J. Mar. Syst. 20, 423–442. https://doi.org/10.1016/S0924-7963(98)00078-5.
Millot, C., 2014. Heterogeneities of in-and out-flows in the Mediterranean Sea. Prog. Oceanogr. 120, 254–278. https://doi.org/10.1016/j.pocean.2013.09.007.
Morales, J.A., 1997. Evolution and facies architecture of the mesotidal Guadiana River delta (S.W. Spain-Portugal). Mar. Geol. 138, 127–148. https://doi.org/10.1016/S0025-3227(97)00009-1.
Morales, J.A., Delgado, I., Gutierrez-Mas, J.M., 2006. Sedimentary characterization of bed types along the Guadiana estuary (SW Europe) before the construction of the Alqueva dam. Estuar. Coast. Shelf Sci. 70, 117–131. https://doi.org/10.1016/j.ecss.2006.05.049.
Moreno, E., Thouveny, N., Delanghe, D., McCave, I.N., Shackleton, N.J., 2002. Climatic and oceanographic changes in the Northeast Atlantic reflected by magnetic properties of sediments deposited on the Portuguese margin during the last 340 ka. Earth Planet. Sci. Lett. 202, 465–480. https://doi.org/10.1016/S0012-821X(02)00787-2.
Moulin, C., Lambert, C.E., Dulac, F., Dayan, U., 1997. Control of atmospheric export of dust from North Africa by the North Atlantic Oscillation. Nature 387, 691–694. https://doi.org/10.1038/42679.
Mulder, T., Lecroart, T.P., Voisset, M., Schönfeld, J., Le Drezen, E., Gonthier, E., Hanquiez, V., Zahn, R., Faugères, J.-C., Hernandez-Molina, F.J., Llave-Barranco, E., Gervais, A., 2002. Past deep-ocean circulation and the paleoclimate record-Gulf of Cadiz. EOS Trans. Am. Geophys. Union 83, 481. https://doi.org/10.1029/2002EO000337.
Mulder, T., Voisset, M., Lecroart, P., Le Drezen, E., Gonthier, E., Hanquiez, V., Faugères, J.C., Habgood, E., Hernandez-Molina, F.J., Estrada, F., Llave-Barranco, E., Poirier, D., Gorini, C., Fuchey, Y., Voelker, A., Freitas, P., Sanchez, F.L., Fernandez, L.M., Kenyon, N.H., Morel, J., 2003. The Gulf of Cadiz: an unstable giant contouritic levee. Geo-Mar. Lett. 23, 7–18. https://doi.org/10.1007/s00367-003-0119-0.
Mulder, T., Lecroart, P., Hanquiez, V., Marches, E., Gonthier, E., Guedes, J.-C., Thiébot, E., Jaaidi, B., Kenyon, N., Voisset, M., Perez, C., Sayago, M., Fuchey, Y., Bujan, S., 2006. The western part of the Gulf of Cadiz: contour currents and turbidity currents interactions. Geo-Mar. Lett. 26, 31–41. https://doi.org/10.1007/s00367-005-0013-z.
Mulder, T., Hassan, R., Ducassou, E., Zaragosi, S., Gonthier, E., Hanquiez, V., Marchès, E., Toucanne, S., 2013. Contourites in the Gulf of Cadiz: a cautionary note on potentially ambiguous indicators of bottom current velocity. Geo-Mar. Lett. 33, 357–367. https://doi.org/10.1007/s00367-013-0332-4.
Nebout, N.C., Peyron, O., Dormoy, I., Desprat, S., Beaudouin, C., Kotthoff, U., Marret, F., 2009. Rapid climatic variability in the West Mediterranean during the last 25 000 years from high resolution pollen data. Clim. Past 5, 19. https://doi.org/10.5194/cp-5-503-2009.
Nelson, C.H., Maldonado, A., 1999. The Cadiz margin study off Spain: an introduction. Mar. Geol. 155, 3–8. https://doi.org/10.1016/S0025-3227(98)00138-8.
Nelson, C.H., Baraza, J., Maldonado, A., 1993. Mediterranean undercurrent sandy contourites, Gulf of Cadiz, Spain. Sediment. Geol. 82, 103–131. https://doi.org/10.1016/0037-0738(93)90116-M.
Nishida, N., 2016. Microstructure of muddy contourites from the Gulf of Cádiz. Mar. Geol. 377, 110–117. https://doi.org/10.1016/j.margeo.2015.08.017.
Ochoa, J., Bray, N., 1991. Water mass exchange in the Gulf of Cadiz. Deep Sea Res. Part Oceanogr. Res. Pap. 38, S465–S503. https://doi.org/10.1016/S0198-0149(12)80021-5.
Oliveira, A., Rocha, F., Rodrigues, A., Jouanneau, J., Dias, A., Weber, O., Gomes, C., 2002. Clay minerals from the sedimentary cover from the Northwest Iberian shelf. Prog. Oceanogr. 52, 233–247. https://doi.org/10.1016/S0079-6611(02)00008-3.
Palanques, A., Diaz, J., Farran, M., 1995. Contamination of heavy metals in the suspended and surface sediment of the Gulf of Cadiz (Spain): the role of sources, currents, pathways and sinks. Oceanol. Acta 18, 469–477. https://archimer.ifremer.fr/doc/00097/20791/.
Palma, C., Oliveira, A., Filali, A., Valenca, M., Mhammdi, N., 2012. Geochemical characteristics of water and sediment in summer period of the Loukkos and Sebou estuaries (NW Morocco): Preliminary study. Bull. L'Institut Sci. Sect. Sci. Terre 34, 69–77.
Peliz, Á., Dubert, J., Santos, A.M.P., Oliveira, P.B., Le Cann, B., 2005. Winter upper ocean circulation in the Western Iberian Basin—Fronts, Eddies and Poleward Flows: an overview. Deep Sea Res. Part Oceanogr. Res. Pap. 52, 621–646. https://doi.org/10.1016/j.dsr.2004.11.005.
Peliz, A., Marchesiello, P., Santos, A.M.P., Dubert, J., Teles-Machado, A., Marta-Almeida, M., Le Cann, B., 2009. Surface circulation in the Gulf of Cadiz: 2. Inflow-outflow coupling and the Gulf of Cadiz slope current. J. Geophys. Res. 114, C03011. https://doi.org/10.1029/2008JC004771.
Petschick, R., 2000. MacDiff 4.2. 5.
Petschick, R., 2002. Röntgendiffraktometrie in der Sedimentologie (K5). Sediment Schriftenr Dtsch Geol Ges 18, 99–118.
Pierce, J.W., Stanley, D.J., 1975. Suspended-sediment concentration and mineralogy in the central and western Mediterranean and mineralogic comparison with bottom sediment. Mar. Geol. 19, M15–M25. https://doi.org/10.1016/0025-3227(75)90053-5.
Pinardi, N., Cessi, P., Borile, F., Wolfe, C.L.P., 2019. The mediterranean sea overturning circulation. J. Phys. Oceanogr. 49, 1699–1721. https://doi.org/10.1175/JPO-D-18-0254.1.
Relvas, P., Barton, D.B., 2002. Mesoscale patterns in the Cape São Vicente (Iberian Peninsula) upwelling region. J. Geophys. Res. 107, 3164. https://doi.org/10.1029/2000JC000456.
Rodrigues, S., Roque, C., Hernández-Molina, F.J., Llave, E., Terrinha, P., 2020. The Sines contourite depositional system along the SW Portuguese margin: Onset, evolution and conceptual implications. Mar. Geol. 430, 106357 https://doi.org/10.1016/j.margeo.2020.106357.
Rogerson, M., Rohling, E.J., Weaver, P.P.E., Murray, J.W., 2005. Glacial to interglacial changes in the settling depth of the Mediterranean Outflow plume. Paleoceanography 20. https://doi.org/10.1029/2004PA001106.
Rogerson, M., Rohling, E.J., Bigg, G.R., Ramirez, J., 2012. Paleoceanography of the Atlantic-Mediterranean exchange: Overview and first quantitative assessment of climatic forcing. Rev. Geophys. 50 https://doi.org/10.1029/2011RG000376.
Rohling, E.J., Marino, G., Grant, K.M., 2015. Mediterranean climate and oceanography, and the periodic development of anoxic events (sapropels). Earth-Sci. Rev. 143, 62–97. https://doi.org/10.1016/j.earscirev.2015.01.008.
Roque, C., Duarte, H., Terrinha, P., Valadares, V., Noiva, J., Cachão, M., Ferreira, J., Legoinha, P., Zitellini, N., 2012. Pliocene and Quaternary depositional model of the

Algarve margin contourite drifts (Gulf of Cadiz, SW Iberia): Seismic architecture, tectonic control and paleoceanographic insights. Mar. Geol. 303–306, 42–62. https://doi.org/10.1016/j.margeo.2011.11.001.

Roque, D., Parras-Berrocal, I., Bruno, M., Sánchez-Leal, R., Hernández-Molina, F.J., 2019. Seasonal variability of intermediate water masses in the Gulf of Cádiz: implications of the Antarctic and subarctic seesaw. Ocean Sci. 15, 1381–1397. https://doi.org/10.5194/os-15-1381-2019.

Rosa, F., Dias, J.A., Mendes, I., Ferreira, Ó., 2011. Mid to late Holocene constraints for continental shelf mud deposition in association with river input: the Guadiana Mud Patch (SW Iberia). Geo-Mar. Lett. 31, 109–121. https://doi.org/10.1007/s00367-010-0219-6.

Sánchez-Goñi, M.F., Cacho, I., Turon, J.L., Guiot, J., Sierro, F.J., Peypouquet, J.-P., Grimalt, J.O., Shackleton, N.J., 2002. Synchroneity between marine and terrestrial responses to millennial scale climatic variability during the last glacial period in the Mediterranean region. Clim. Dyn. 19, 95–105. https://doi.org/10.1007/s00382-001-0212-x.

Sánchez-Leal, R.F., Bellanco, M.J., Fernández-Salas, L.M., García-Lafuente, J., Gasser-Rubinat, M., González-Pola, C., Hernández-Molina, F.J., Pelegrí, J.L., Peliz, A., Relvas, P., Roque, D., Ruiz-Villarreal, M., Sammartino, S., Sánchez-Garrido, J.C., 2017. The mediterranean overflow in the gulf of cadiz: a rugged journey. Sci. Adv. 3, eaao0609. https://doi.org/10.1126/sciadv.aao0609.

Schönfeld, J., 1997. The impact of the Mediterranean Outflow Water (MOW) on benthic foraminiferal assemblages and surface sediments at the southern Portuguese continental margin. Mar. Micropaleontol. 29, 211–236. https://doi.org/10.1016/S0377-8398(96)00050-3.

Schönfeld, J., Zahn, R., 2000. Late Glacial to Holocene history of the Mediterranean Outflow. Evidence from benthic foraminiferal assemblages and stable isotopes at the Portuguese margin. Palaeogeogr. Palaeoclimatol. Palaeoecol. 159, 85–111. https://doi.org/10.1016/S0031-0182(00)00035-3.

Shiozowa, T., 1970. The experimental study on differential floculation of clay minerals - an application of its results in recent sediments of Ishikari Bay. J. Jpn. Assoc. Mineral. Petrol. Econ. Geol. 63, 75–84. https://doi.org/10.2465/ganko1941.63.75.

Sierro, F.J., Flores, J.A., Baraza, J., 1999. Late glacial to recent paleoenvironmental changes in the Gulf of Cadiz and formation of sandy contourite layers. Mar. Geol. 155, 157–172. https://doi.org/10.1016/S0025-3227(98)00145-5.

Skonieczny, C., Bory, A., Bout-Roumazeilles, V., Abouchami, W., Galer, S.J.G., Crosta, X., Stuut, J.-B., Meyer, I., Chiapello, I., Podvin, T., Chatenet, B., Diallo, A., Ndiaye, T., 2011. The 7–13 March 2006 major Saharan outbreak: multiproxy characterization of mineral dust deposited on the West African margin. J. Geophys. Res. 116, D18210. https://doi.org/10.1029/2011JD016173.

Skonieczny, C., Bory, A., Bout-Roumazeilles, V., Abouchami, W., Galer, S.J.G., Crosta, X., Diallo, A., Ndiaye, T., 2013. A three-year time series of mineral dust deposits on the West African margin: Sedimentological and geochemical signatures and implications for interpretation of marine paleo-dust records. Earth Planet. Sci. Lett. 364, 145–156. https://doi.org/10.1016/j.epsl.2012.12.039.

Snoussi, M., 1986. Nature, estimation et comparaison des flux de matières issus des bassins versants de l'Adour (France), du Sébou, de l'Oum-Er-Rbia et du Souss (Maroc). In: Impact du Climat sur les Apports Fluviatiles à l'océan. Université de Bordeaux I, Bordeaux.

Solari, S., Egüen, M., Polo, M.J., Losada, M.A., 2017. Peaks over Threshold (POT): a methodology for automatic threshold estimation using goodness of fit p-value. Water Resour. Res. 53, 2833–2849. https://doi.org/10.1002/2016WR019426.

Stow, D.A.V., Faugères, J.-C., Gonthier, E., 1986. Facies distribution and textural variation in Faro Drift contourites: velocity fluctuation and drift growth. Mar. Geol. 72, 71–100. https://doi.org/10.1016/0025-3227(86)90100-3.

Stow, D.A.V., Hernández-Molina, F.J., Llave, E., Bruno, M., García, M., Díaz del Rio, V., Somoza, L., Brackenridge, R.E., 2013a. The cadiz contourite channel: sandy contourites, bedforms and dynamic current interaction. Mar. Geol. 343, 99–114. https://doi.org/10.1016/j.margeo.2013.06.013.

Stow, D.A.V., Hernández-Molina, F.J., Llave, E., Bruno, M., García, M., Díaz del Rio, V., Somoza, L., Brackenridge, R.E., 2013b. The cadiz contourite channel: sandy contourites, bedforms and dynamic current interaction. Mar. Geol. 343, 99–114. https://doi.org/10.1016/j.margeo.2013.06.013.

Stumpf, R., Frank, M., Schönfeld, J., Haley, B.A., 2011. Climatically driven changes in sediment supply on the SW Iberian shelf since the last Glacial Maximum. Earth Planet. Sci. Lett. 312, 80–90. https://doi.org/10.1016/j.epsl.2011.10.002.

Stuut, J.-B., Smalley, I., O'Hara-Dhand, K., 2009. Aeolian dust in Europe: African sources and European deposits. Quat. Int. 198, 234–245. https://doi.org/10.1016/j.quaint.2008.10.007.

Teixeira, M., Terrinha, P., Roque, C., Rosa, M., Ercilla, G., Casas, D., 2019. Interaction of alongslope and downslope processes in the Alentejo margin (SW Iberia) – Implications on slope stability. Mar. Geol. 410, 88–108. https://doi.org/10.1016/j.margeo.2018.12.011.

Thiry, M., 2000. Palaeoclimatic interpretation of clay minerals in marine deposits: an outlook from the continental origin. Earth-Sci. Rev. 49, 201–221. https://doi.org/10.1016/S0012-8252(99)00054-9.

Toucanne, S., Mulder, T., Schönfeld, J., Hanquiez, V., Gonthier, E., Duprat, J., Cremer, M., Zaragosi, S., 2007. Contourites of the Gulf of Cadiz: a high-resolution record of the paleocirculation of the Mediterranean outflow water during the last 50,000 years. Palaeogeogr. Palaeoclimatol. Palaeoecol. 246, 354–366. https://doi.org/10.1016/j.palaeo.2006.10.007.

Turon, J.-L., Lézine, A.-M., Denèfle, M., 2003. Land–sea correlations for the last glaciation inferred from a pollen and dinocyst record from the Portuguese margin. Quat. Res. 59, 88–96. https://doi.org/10.1016/S0033-5894(02)00018-2.

Vale, C., Sundby, B., 1987. Suspended sediment fluctuations in the Tagus estuary on semi-diurnal and fortnightly time scales. Estuar. Coast. Shelf Sci. 25, 495–508. https://doi.org/10.1016/0272-7714(87)90110-7.

van Dijk, J., Ziegler, M., de Nooijer, L.J., Reichart, G.J., Xuan, C., Ducassou, E., Bernasconi, S.M., Lourens, L.J., 2018. A saltier glacial mediterranean outflow. Paleoceanogr. Paleoclimatol. 33, 179–197. https://doi.org/10.1002/2017PA003228.

Van Geen, A., Adkins, J.F., Boyle, E., Nelson, C.H., Palanques, A., 1997. A 120-yr record of widespread contamination from mining of the Iberian pyrite belt. Geology 25, 291–294. https://doi.org/10.1130/0091-7613(1997)025<0291:AYROWC>2.3.CO;2.

Vergnaud-Grazzini, C., Calarp, M., Faugères, J.-C., Gonthier, E., Grousset, F., Pujol, C., Saliège, J.-F., 1989. Mediterranean outflow through the Strait of Gibraltar since 18 000 years BP. Oceanol. Acta 12, 305–324.

Voelker, A., Lebreiro, S., Schonfeld, J., Cacho, I., Erlenkeuser, H., Abrantes, F., 2006. Mediterranean outflow strengthening during northern hemisphere coolings: a salt source for the glacial Atlantic? Earth Planet. Sci. Lett. 245, 39–55. https://doi.org/10.1016/j.epsl.2006.03.014.

Voelker, A.H.L., 2015. Oxygen and hydrogen isotope signatures of Northeast Atlantic water masses. Deep Sea Res. Part II Top. Stud. Oceanogr. 116, 89–106. https://doi.org/10.1016/j.dsr2.2014.11.006.

Voelker, A.H.L., Rodrigues, T., Billups, K., Oppo, D., McManus, J., Stein, R., Hefter, J., Grimalt, J.O., 2010. Variations in mid-latitude North Atlantic surface water properties during the mid-Brunhes (MIS 9–14) and their implications for the thermohaline circulation. Clim. Past 6, 531–552. https://doi.org/10.5194/cp-6-531-2010.

Waelbroeck, C., Labeyrie, L., Michel, E., Duplessy, J.C., McManus, J.F., Lambeck, K., Balbon, E., Labracherie, M., 2002. Sea-level and deep water temperature changes derived from benthic foraminifera isotopic records. Quat. Sci. Rev. 21, 295–305. https://doi.org/10.1016/S0277-3791(01)00101-9.

Whitehouse, U.G., Jeffrey, L.M., Debrecht, J.D., 1960. Differential settling tendencies of clay minerals in saline water. Clay Clay Miner. 1–79 https://doi.org/10.1016/B978-0-08-009235-5.50006-1.